Published in final edited form as:
Annu Rev Physiol. 2003 ; 65: 851–879.

G Protein-Coupled Receptor Rhodopsin: A Prospectus

Sławomir Filipek[1], **Ronald E. Stenkamp**[2,7], **David C. Teller**[3,7], and **Krzysztof Palczewski**[4,5,6]
1*Department of Chemistry, University of Warsaw, 1 Pasteur St, PL-02093 Warsaw, Poland*

2*Department of Biological Structure, University of Washington, Seattle, Washington 98195*

3*Department of Biochemistry, University of Washington, Seattle, Washington 98195*

4*Department of Ophthalmology, University of Washington, Seattle, Washington 98195*

5*Department of Chemistry, University of Washington, Seattle, Washington 98195*

6*Department of Pharmacology, University of Washington, Seattle, Washington 98195 e-mail: palczews@u.washington.edu*

7*Department of Biomolecular Structure Center, University of Washington, Seattle, Washington 98195*

Abstract

Rhodopsin is a retinal photoreceptor protein of bipartite structure consisting of the transmembrane protein opsin and a light-sensitive chromophore 11-*cis*-retinal, linked to opsin via a protonated Schiff base. Studies on rhodopsin have unveiled many structural and functional features that are common to a large and pharmacologically important group of proteins from the G protein-coupled receptor (GPCR) superfamily, of which rhodopsin is the best-studied member. In this work, we focus on structural features of rhodopsin as revealed by many biochemical and structural investigations. In particular, the high-resolution structure of bovine rhodopsin provides a template for understanding how GPCRs work. We describe the sensitivity and complexity of rhodopsin that lead to its important role in vision.

Keywords

crystal structure; phototransduction; vitamin A; transmembrane protein; vision; signal transduction

INTRODUCTION: HISTORICAL PERSPECTIVE

The visual pigment rhodopsin was originally extracted from bovine retina using bile salts by Kühne (1). He found that the color of rhodopsin resulted from a chromophore different from xanthophylls (egg yolk) or β-carotene (corpus luteum). It faded upon exposure to light, heating, or organic solvents and could be salted out from the extract by ammonium sulfate. Regeneration of bleached rhodopsin required interaction of the retina with adjacent retinal pigment epithelium cells (RPE). The need for vitamin A in vision triggered an interest in retinoids as a potential source of the chromophore. Wald provided evidence that visual pigment is composed of a protein conjugated with an unidentified retinoid (2). Vitamin A (all-*trans*-retinol) is a precursor of this retinoid and a product of visual pigment photobleaching. Successive work demonstrated that bleaching and regeneration of the visual pigment involves a cycle of stereoisomerization of all-*trans*-retinal/all-*trans*-retinol. The reddish color of rhodopsin results from the protonated Schiff base linkage of 11-*cis*-retinal to the membrane protein opsin (3,4).

The *Annual Review of Physiology* is online at http://physiol.annualreviews.org

Therefore, a metabolic cycle of production and recycling of the photoisomerized visual chromophore is essential for our vision. Bleaching of rhodopsin introduces a succession of quasi-stable intermediates that within milliseconds reach an equilibrium of metarhodopsin I (Meta I) and metarhodopsin II (Meta II) (5). Meta II is favorable in higher temperatures and pH, salt, and glycerol, and its formation is accompanied by a large increase in entropy. Subsequent work focused on bovine rhodopsin, where the naturally high abundance of this interesting protein was utilized in a number of biochemical and biophysical approaches [early work reviewed in (6)].

The first protein amino acid sequence of the G protein-coupled receptor (GPCR), opsin, was determined in the laboratories of Hargrave et al. and Ovchinnikov (7,8), and the first models of the seven-transmembrane helix topology, based partly on proteolysis, antibody-recognition, and chemical and posttranslational (glycosylation) modifications, were introduced (9). The overall topology of rhodopsin is similar to another retinylidene-binding protein, bacteriorhodopsin (8). In parallel with the improved understanding of the properties of rhodopsin, functional studies provided a solid basis for the way the light signal is translated into biochemical reactions, a process termed phototransduction. Fung & Stryer demonstrated that light-activated rhodopsin catalyzes the nucleotide exchange of GDP to GTP in an interacting protein called transducin, a G protein, which in turn activates a photoreceptor cGMP-specific phosphodiesterase (10). Hundreds of transducin molecules are activated per photoactivated rhodopsin in this first amplification step during phototransduction (11). Deprotonation of Meta II's Schiff base between the chromophore and opsin appeared to be critical for the activating property of light-exposed rhodopsin (12). A fortuitous discovery, made in the early 1970s, that rhodopsin is phosphorylated (13-15), has been connected with observations that ATP mediates quenching of phosphodiesterase activity (16,17). The responsible rhodopsin kinase has been purified (18) and cloned (19). For complete quenching of the light-activated phosphorylated rhodopsin activity, specific binding of a 48-kDa protein is critical (20). Arrestin-like molecules play a key role in the signaling and cellular processes of a large number of agonist-stimulated GPCRs (21).

Nathans & Hogness were the first to clone opsin from the bovine cDNA library (22). Subsequently, the generated bovine DNA sequence was essential in the determination of the bovine opsin genomic structure (22); the determination of the cDNA and genomic structures of human opsin and blue, green, and red visual pigments (23,24); the cloning of the first invertebrate rhodopsin and its gene from *Drosophila* (25); and the total chemical synthesis of cDNA for bovine rhodopsin (26).

The crystal structure of rhodopsin isolated from bovine retinas has been solved (27) and refined (28), providing significant insight into the function of this important molecule. In this review, we describe the major structural properties of rhodopsin. As with any rich subject, not all of the nuances of rhodopsin structure and function can be covered here. Therefore, the authors encourage readers to peruse other reviews dedicated to rhodopsin and different aspects of phototransduction (6,21,29-36).

RHODOPSIN

Expression

Retinal rod cells are specialized neurons that function in capturing photons and communicating with secondary neurons about the presence of light. These events are initiated by conformational changes in the light-sensitive pigment, rhodopsin, followed by a biochemical cascade of reactions, termed phototransduction (30,31). In mammalian retina there are ~10^8 photoreceptor cells. Rods are highly differentiated cells with outer segments (ROS) containing all components necessary for phototransduction. ROS are composed of stacks of 1000–2000

independent disk membranes surrounded by plasma membrane (Figure 1, see Supplemental Materials: Follow the Supplemental Material link on the Annual Reviews homepage at http://annualreviews.org/). The main component of the disk membranes is rhodopsin (>90% of the membrane's proteins). Opsin, the protein component of rhodopsin, is specifically expressed in retinal rod photoreceptors and in some cells of the pineal gland (37). In adult mice, 0.06% of the total retinal RNA encodes for opsin (photoreceptors constitute ~80–90% of all cells in the retina) (38). This translates into the highest expression of any GPCR. About 0.5–1 mg of rhodopsin can be isolated from one bovine retina.

Purification

The absorption spectrum of rhodopsin in detergent solutions displays two maxima in the UV-Vis region: the protein band around 280 nm and the chromophore-related peak at 498 nm. The ratio of the absorption $A_{280\ nm}/A_{498\ nm}$ for pure rhodopsin devoid of opsin is ~1.6, with an extinction coefficient of 42,000 $cm^{-1}\ M^{-1}$ at 498 nm. Rhodopsin is stable at room temperature for days when extracted into many detergents, including Chaps, dodecyl-β-maltoside, or Tween 80. The most frequent source of native rhodopsin is bovine eyes. Native rhodopsin is initially pre-purified by isolation of ROS from the retina using a sucrose gradient method (50–70% rhodopsin content in ROS) [reviewed in (6)]. The purification methods require separation of rhodopsin from contaminating proteins and from bleached opsin. All methods require detergent for rhodopsin solubilization. The first method takes advantage of rhodopsin glycosylation and employs concanavalin A affinity chromatography (39). A large percent of opsin binds irreversibly to the resin. Concanavalin A chromatography is scalable, and large amounts of material can be prepared, although the purified rhodopsin is contaminated with other glycoproteins and with concanavalin A, which leaches from the resin. The second method uses hydroxyapatite chromatography and yields only partially purified protein (40). Rhodopsin is also efficiently purified by immunoaffinity chromatography using Molday's 1D4 monoclonal antibody, which recognizes seven to nine C-terminal amino acids of bovine rhodopsin. This method is particularly useful for heterologously expressed rhodopsin and other visual pigments (26,41). The fourth method takes advantage of highly enriched rhodopsin in ROS and the instability of opsin and contaminating protein during prolonged incubation in mild detergent in the presence of divalent metal ions (43). It is an effective and scalable method that does not use any chromatographic columns. This method also enriches rhodopsin preparations with native ROS lipids and produces highly concentrated rhodopsin with controllable concentrations of detergent suitable for crystallization studies. This method is not applicable to heterologous systems due to the low expression levels of rhodopsin.

Composition

Rhodopsin is composed of a transmembrane apoprotein, opsin, and 11-*cis*-retinal bound to the protein through a Schiff base linkage to a lysine side-chain. Bovine opsin (Swiss-Prot: P02699) is composed of 348 amino acids with a molecular mass of 39,007. The total molecular mass increases to 42,002 when posttranslational modifications are included (palmitoylation, acetylation of N terminus, and glycosylation). The most prevalent amino acids are Phe (8.9%), Val (8.9), Ala (8.3), and Leu (8.0), suggesting a major hydrophobic character for this protein.

Rhodopsin is extensively modified by posttranslational modifications. The chromophore is attached through a protonated Schiff base to Lys^{296} (44). The N-terminal Met is acetylated (45), as is found frequently for other eukaryotic proteins at their initiation Met residue. Using ex vivo [^{3}H]-labeling, it was shown that opsin is palmitoylated (46), a modification that is frequently observed among GPCRs. Two Cys residues, Cys^{322} and Cys^{323} located at the C terminus, are palmitoylated (47). Two Cys residues from helix III and E III (the loop connecting helices IV and V) are cross-linked by a disulfide bond (48). Two $(Man)_3(GlcNAc)_3$ groups modify opsin through an asparagine-linkage (Figure 2, see Supplemental Materials: Follow

the Supplemental Material link on the Annual Reviews homepage at http://annualreviews.org/) at the N terminus (Asn^2 and Asn^{15}) (49). Glycosylation is not homogenous and other, but minor, compositions of the carbohydrate moieties were identified (50). Rhodopsin undergoes a light-dependent phosphorylation on six to seven Ser/Thr residues at the C-terminal end (51). In vivo, there are three sites, Ser^{336}, Ser^{338}, and Ser^{343}, that are phosphorylated by direct and quantitative methods after 20–40% bleaching of the protein (52,53). The phosphorylation processes, at lower bleaches such as 100–10,000 photons/s per rod, are not yet accessible to currently available technologies. At these bleach levels, our rods are functional before they saturate at more intense light. Heterogeneity and multiple rhodopsin phosphorylation have been observed in vitro [reviewed in (54)].

Rhodopsin, when isolated from ROS, contains variable amounts of tightly bound phospholipids. These lipids possibly stabilize rhodopsin and coat the hydrophobic transmembrane regions of the protein. We found, using radioactive phospholipids, that they can be removed completely only under very harsh conditions, such as 1% SDS in formic acid and trifluoroethanol (1:1) (X. Zhou & K. Palczewski, unpublished data). It is reasonable to speculate that the integrity of rhodopsin and other membrane proteins may be lost by removal of all tightly associated lipids.

Regeneration and Photobleaching Pathway

The key reaction of visual excitation is the ultra-fast (femtoseconds) photochemical reaction of rhodopsin's chromophore, 11-*cis*-retinal forming all-*trans*-retinal (55). From a theoretical organic chemistry point of view, this isomerization most likely involves the “Hula-Twist” mechanism that preserves, at first approximation, the positions of theβ-ionone ring and the Schiff base (56). A conventional “one-bond-flip” mechanism would predict a large rotation of the β-ionone ring within the rhodopsin molecules (Figure 3, see Supplemental Materials: Follow the Supplemental Material link on the Annual Reviews homepage at http://annualreviews.org/). In milliseconds, the signaling Meta II is established and this catalytically active form of rhodopsin binds and activates transducin (T, G_t).

The photoisomerization of 11-*cis*-retinylidene to all-*trans*-retinylidene triggers conformational changes of opsin through multiple intermediates, such as photorhodopsin, bathorhodopsin, lumirhodopsin, Meta I, Meta II, and Meta III, before the chromophore hydrolyzes and leaves the binding pocket (34). These intermediates are short-lived, but can be trapped by low temperature and distinguished by specific absorption maxima in the range of visible light (57). The final steps, namely hydrolysis of all-*trans*-retinylidene and its relation to Meta III, are poorly understood at the mechanistic level. The hydrolysis of the Schiff base appears to be the rate-limiting step in the release of the chromophore (58). In addition, two forms of Meta II were identified, Meta IIa and Meta IIb, that differ in the protonation state at the cytoplasmic surface, whereas the Schiff base is deprotonated with a characteristicλ_{max} at 380 nm (59). The transducin-activating form is Meta IIb (34).

Free all-*trans*-retinal also binds to opsin and forms partially active receptors toward activation of transducin [reviewed in (60)]. This activity is enhanced compared with the activity of free opsin. From the crystallographic model, a potential binding site for the retinal has been identified in the hydrophobic domain of rhodopsin (D.C. Teller, unpublished data). For 11-*cis*-retinal, binding to this site could be the first step in the regeneration of rhodopsin, before the chromophore binds non-covalently to the retinylidene cavity and prior to stable formation of the Schiff base (61). In the Meta II-transducin complex, all-*trans*-retinylidene can be photoisomerized back to 11-*cis*-retinylidene without transducin dissociation, suggesting that the G protein imposes conformational changes on the rhodopsin surface that cannot be reversed even upon photoisomerization (62). However, when Meta II is photolyzed by blue light, a product is formed that has absorption properties similar to that of rhodopsin with λ_{max} at 500

nm, but with all-*trans*-retinal bound (63). These data indicate that all-*trans*-retinylidene can be bound in the transmembrane segment of rhodopsin in two distinct conformations: one that activates the opsin moiety and another that inactivates it.

Mutagenesis

Availability of rhodopsin sequences and development of molecular biology techniques have had tremendous impacts in probing rhodopsin structure using muta-genesis and biochemical approaches. Findings from this research are discussed in the subsequent paragraphs, where they strengthen observations and interpretation of rhodopsin's structure and function.

A general method for rhodopsin expression and purification from monkey (or human) kidney cells (64), insect cells (65), and different yeast strains (66,67) was introduced. In particular, we benefited from these studies in understanding the spectral tuning of rhodopsin. Retinals in their Schiff base forms absorb in the near ultraviolet range (360–380 nm, compared with ~320 nm for retinols). The predicted counterion for the protonated Schiff base has been identified as Glu^{113}, which is highly conserved among all known vertebrate visual pigments (68-70). The addition of a proton to the Schiff base, together with critical placement of intramolecular negative charges, results in a bathochromic shift in the absorption spectrum to that characteristic of native rhodopsin (500 nm). The counterion in the hydrophobic environment causes a ~sevenfold increase in the pK_a of the protonated Schiff base. Therefore, rhodopsin in its native environment will have its chromophore in the protonated Schiff base linkage (29).

Glycosylation was shown to be dispensable for the proper folding and function of rhodopsin. Mutant rhodopsins lacking Asn^{15}-glycosylation exhibited poor folding and were defective in transport to the cell surface. They were also poor transducin activators, perhaps owing to their intrinsic instability (71). These studies have not yet been extended to mouse animal models.

Ridge et al. pioneered studies of rhodopsin using expressed polypeptide fragments in COS cells. Splitting rhodopsin in the second and third cytoplasmic loops led to production of two-fragment rhodopsins that show properties similar to the wild-type (72,73). These studies, and earlier limited proteolysis studies [reviewed in (6)], revealed several important aspects of rhodopsin function. For example, connecting subsequent loops II and III have only a small stabilizing effect on rhodopsin, whereas the chromophore is critical for the stabilization of the tertiary structure. It appears that helices I–III and V–VII, with helix IV connected to either of these two fragments, form active rhodopsin, suggesting the existence of two independent intradomain interactions. These data are in agreement with another set of experiments. Rhodopsin retains its spectrum after extensive proteolysis of its exposed loops by pronase in native membranes, or in detergent solutions, albeit, digested rhodopsin is more temperature-sensitive to denaturation (K. Palczewski, unpublished data).

CRYSTAL STRUCTURE OF RHODOPSIN

Crystallization and Data Analysis

Rhodopsin was selectively extracted from highly purified bovine ROS using a mild detergent (such as nonyl-β-glucoside) and high concentrations of divalent metal ions (for example, 80 mM Zn^{2+}) in the absence of Cl^- ions. This method, developed by a postdoctoral fellow, T. Okada, therefore does not involve any column chromatography and maintains high concentrations of endogenous lipids in the extract (43). Importantly, pre-incubation of ROS at room temperature in detergent causes opsin and other membranous proteins to precipitate and be efficiently separated from rhodopsin. Opsin is present up to 15% of total opsin and rhodopsin in cow eyes obtained from a local slaughterhouse. The purified rhodopsin had an $A_{280\ nm}/A_{500\ nm}$ ratio of 1.6, close to the theoretical minimum of 1.5, suggesting high purity of the protein and a lack of bleached rhodopsin, opsin (43,74). Vapor diffusion crystallization

techniques were used to crystallize rhodopsin, using ammonium sulfate as the precipitant and heptane-1,2,3-triol as an additive in nonyl-β-glucoside detergent solutions. Diffraction quality crystals were obtained and all were merohedrally twinned to different degrees (43). The crystals were also sensitive to visible light (75). To avoid bleaching, all procedures were performed under dim red-light illumination. Initial diffraction data for the native protein were collected at Stanford Synchrotron Radiation Laboratory and Advanced Photon Source synchrotrons; however, attempts to solve the structure using bacteriorhodopsin as a molecular replacement model failed. Hg-derivatives of rhodopsin were generated for multiple isomorphous replacement (MIR) and multiwave length anomolous dispersion (MAD) phasing experiments. The structure was solved using a six-wavelength mercury MAD data set obtained at SPring8 on a crystal with a 10% twinning ratio by Miyano and colleagues (27). Crystallographic refinement of the two molecules in the asymmetric unit generated the current model of rhodopsin at 2.8 Å resolution (28).

Dimers and Crystallographic Lattice

Rhodopsin molecules, crystallized in space group $P4_1$, are packed in the crystal lattice to form an array of tube-like structures (Figure 1*A*). Eight rhodopsin molecules fill the unit cell, with ~70% of the space occupied by solvent. The dimensions of the unit cell are: a = b = 97.3 Å, c = 149.5 Å. Two copies of rhodopsin (denoted molecules A and B) make up the asymmetric unit and are related by a non-crystallographic twofold axis between helices IA and IB. The crystallographic lattice is formed by remarkably few contacts between the molecules when compared with an unrelated, but also seven-transmembrane helical protein, sensory rhodopsin, crystallized by a lipid cubic phase method (Figure 1*B*) (76).

The dimer of rhodopsin, as seen in the crystal structure, cannot be physiologically relevant, as one molecule is rotated by ~160° in relation to the second. The two cytoplasmic surfaces (Figure 4, see Supplemental Materials: Follow Supplemental Materials link on Annual Reviews homepage at http://annualreviews.org/) would project toward opposite sides of the membrane if this arrangement were found in the bilayer. One of these two rhodopsins makes much fewer contacts than the other in the crystal. It appears that a strong hydrophobic interaction between rhodopsin molecules allows elongation of the dimers in the crystal, with only one molecule promoting the tube-like structure while the other piggybacks in the dimer. The two sets of interacting residues found for molecules A and B are not identical because of asymmetry in the dimer and slightly different protein conformations for the two crystallographically independent molecules (Figure 4*A*, Suppl. Figure). These interactions may possibly deform the structure of rhodopsin to some degree; however, preservation of rhodopsin's spectral properties suggests that any disorder would be localized and not affect the binding site of the chromophore. The contacts between dimers also occur with different residues in molecules A and B (Figure 4*A*, Suppl. Figure). In addition, these contacts involve the oligosaccharides bound to the protein (Figure 4*A–C*, Suppl. Figure).

Three-Dimensional Model

The current model of bovine rhodopsin (Figure 2) includes >95% of its amino acid residues. Missing residues in the structure are $Gln^{236}GlnGlnGluSer^{240}$ and $Asp^{331}GluAla^{333}$ in molecule A; and $Lys^{141}ProMetSerAsnPheArgPhe^{148}$, $Val^{227}PheThrValLysGluAlaAlaAlaGlnGlnGlnGluSerAlaThrThr^{243}$, and $Pro^{327}LeuGlyAspAspGluAlaSerThrThrValSerLysThrGluThrSerGlnValAlaProAla^{348}$ in molecule B. The shape of the transmembrane domain is that of an elliptic cylinder of width ~41 Å, height ~75 Å. The length and width of the elliptic footprint on the plane at the middle of the membrane is roughly 45 by 37 Å. Rhodopsin, when projected on the membrane, occupies a surface close to 1500 $Å^2$ (28). Two palmitoyl chains have been identified and two oligosaccharide units have been modeled. Rhodopsin folds into seven transmembrane helices,

I–VII, varying in length from 22 to 34 residues, and one cytoplasmic helix (Figure 2; helix VIII in red running parallel to imaginary membranes). These helices also differ on the level of irregularities and are tilted at various angles with respect to the expected membrane surface (28). The chromophore occupies a cavity approximately two thirds from the top or cytoplasmic side of the transmembrane segment, a location that had been previously predicted from biophysical studies (77).

The extracellular, doubly glycosylated domain is formed by 33 N-terminal amino acids and by interhelical loops between helices II and III (residues 101–105), IV and V (residues 173–198), and VI and VII (277–285). The region displays a noticeably compact structure. Four distorted short β-strands form a plug that limits accessibility to the chromophore-binding site from this extracellular side. The Gly^{3} to Pro^{12} region forms the first β-hairpin that runs parallel to the expected plane of the membrane. The third and fourth β-strands, Arg^{177} to Asp^{190}, form a second twisted β-hairpin. This region contains the Cys^{187} portion of the disulfide bond. The fourth β-strand is below the 11-*cis*-retinal and is a part of the chromophore-binding pocket with the carbonyl oxygen atom of Cys^{187} being only 3.0 Å from C_{12} of the retinal. An additional consequence of the plug is that Glu^{181}, highly conserved in rhodopsins and in short- to mid-wavelength visual pigments (29), is in close proximity (4.4 Å) to retinal at the C_{12} position. Glu^{181} modulates the stability of Meta II and its accessibility to hydroxylamine (78), suggesting that the plug region prevents rapid dissociation to the intradiscal space. In red visual pigments, a His residue occupies this position, forming a part of the binding site for a Cl^{-} ion (79). A Cl^{-} ion modulates the λ_{max} of the absorption spectrum, causing a bathochromic shift by ~40 nm for these cone visual pigments, compared with pigments in mutants lacking this binding site (80).

The C-terminal structure of rhodopsin does not have any secondary structural elements. From Gly^{324} to Asp^{330}, the polypeptide folds back over cytoplasmic helix VIII. Residues 331–333 have no discernable electron density; therefore, the conformation of this region is uncertain. Functionally, rhodopsin's C terminus plays two roles. It is necessary for the vectorial transport of rhodopsin from the site of synthesis to the rod outer segment (81-83) and for desensitization of photoactivated rhodopsin (35,84).

The cytoplasmic surface contains two short loops connecting helices I and II (residues 65–70), and helices III and IV (residues 141–149). A third cytoplasmic loop is between helices V and VI (residues 226–243). In the current model this loop is incomplete, lacking electron density for residues 236–240. The C terminus is unstructured in solution (85) but likely folds over a loop between helices I and II (86). At the exit of transmembrane helix VII is helix VIII, which is fully cytoplasmic, formed by residues 311–323, and 16 Å in length.

Two-Dimensional Model

A two-dimensional model of rhodopsin (Figure 3) is based on a similar earlier model (9). Fourteen positively charged residues are present on the cytoplasmic surface of rhodopsin, whereas only three are on the extracellular face, in agreement with the positive inside rule for multi-spanning eukaryotic membrane proteins (87). In particular, three positive charges in the first cytoplasmic loop of rhodopsin may be critical for proper insertion into the membranes (88). The negatively charged residues are similar on both sides of the membrane. Nominally, rhodopsin has four charged residues buried in the transmembrane region of rhodopsin: Asp^{83} in helix II, Glu^{113} and Glu^{122} in helix III, and Lys^{296} in helix VII. Two of these residues are engaged in chromophore-binding, one by donating an amino group (Lys^{296}) to form a protonated Schiff base and the other, Glu^{113}, by acting as a counterion for this linkage. Two other charged residues, along with positive and negative residues at the ends of the transmembrane helices, could be involved in the formation of water channels and water

polarization within the hydrophobic interior of the molecule. This inference has yet to be substantiated by strong experimental proof.

A set of residues facing the outside of the molecule are all highly hydrophobic, as expected, either lacking side-chains (Gly), or having a small side chain such as Ala. Surprisingly, five imino-acid residues, Pro, are also facing the lipids (Figure 3; the three-dimensional model is shown in Figure 5, see Supplemental Materials: Follow the Supplemental Material link on the Annual Reviews homepage at http://physiol.annualreviews.org/). The composition of the lipid-facing residues could be important for the formation of an organized oligomeric structure of this transmembrane protein in the lipid bilayer (89).

Helices of Rhodopsin and Interhelical Interactions

Helix I, (encompassing residues 34 through 64 and having a length of 45 Å, is tilted ~25° from the vector perpendicular to the plane of membranes and is bent by 12° around Pro^{53}. The C-terminal tail of rhodopsin occupies the space over part of the helical bundle, helix I and helix VII. Helix I forms multiple hydrogen bond interactions with helices II, VII, and VIII (Figure 4). One of the residues that exhibits the highest conservation among related proteins is Asn^{55} in helix I. Its side chain is responsible for two interhelical hydrogen bonds to Asp^{83} in helix II and to the peptide carbonyl of Ala^{299}. Additional interactions involve Tyr^{43}-Phe^{293} and Asn^{55}-Ala^{299} with helix VII and Gln^{64}-Thr^{320} with helix VIII (Figure 4). These and other hydrophobic interactions are depicted in Figure 6*A* (see Supplemental Materials: Follow the Supplemental Material link on the Annual Reviews homepage at http://physiol.annualreviews.org/).

Helix II, formed by residues 71 through 100, has a length of 40 Å, is tilted ~25° from the vector perpendicular to the plane of membranes, and is bent by 30° around tandem Gly residues, Gly^{89} and Gly^{90}. As a consequence of this bending, Gly^{90} is in the vicinity of Glu^{113}, the counterion for the protonated Schiff base of the chromophore. This helix forms multiple hydrogen bond interactions with helix I (see above), helix III (Asn^{78}–Ser^{127}), and helix IV (Tyr^{74}-Glu^{150}, Asn^{78}-Thr^{160}, Asn^{78}-Trp^{161}) (Figure 4). It appears that it forms a tight pair with helix I owing to extensive hydrophobic interactions, in addition to the ionic interaction between Asn^{55} and Asp^{83} (Figure 4). The cytoplasmic ends of helices II and IV are close to each other.

Helix III, extraordinarily important for rhodopsin, encompasses residues 106 to 139. It is the longest helix at 48 Å in length, tilted ~33° from the vector perpendicular to the plane of membranes, and is bent twice, once by 12° around Gly^{120}-Gly^{121} and the second by 11° at Ser^{127}. The large tilt of this helix results in the helix running across the helical bundle and making contacts with five other helices (II, IV, V, VI, and VII) (Figure 4; Figure 6*A*, see Suppl. Figure). The ionic/hydrogen bond interactions include Asn^{78}-Ser^{127}, Glu^{122}-Trp^{126}-His^{211}, Cys^{140}-Thr^{229}, Arg^{135}-Glu^{247}, and Glu^{113}-Lys^{296} (retinal). At the extracellular end of helix III, Cys^{110} is engaged in a disulfide bond with Cys^{187} of the β-sheet. This disulfide bond is highly conserved among GPCRs. In the middle of this helix, Glu^{113}, Gly^{114}, Ala^{117}, Thr^{118}, Gly^{120}, Gly^{121}, and Gly^{122} run below the β-ionone ring to C_{15} of the chromophore. Glu^{113} is the counterion for the protonated Schiff base formed between retinal and Lys^{296}. The C-terminal end of helix III at the cytoplasmic surface contains the E(D)RY motif located in an extremely hydrophobic environment formed among residues from helices II, IV, V and VI. The E(D)RY residues (although for rhodopsin this motif is ERY, in a majority of GPCRs it is DRY and therefore referred to as the DRY motif) have been implicated in the regulation of the receptor's interaction with its G protein. In this motif, there are salt bridges between Glu^{134}, Glu^{247}, and Arg^{135}. This organization of ionic interactions within the hydrophobic pocket could be one of the critical constraints in keeping rhodopsin in the inactive conformation. The crystal structure in this region has high atomic displacement parameters (B-values), however, and the

side chains may assume different orientations. The DRY motif is highly conserved among GPCRs.

Helix IV, the shortest transmembrane helix, encompasses residues 150 through 172 and is 33 Å in length. It runs almost perpendicular to the plane of the membrane and is bent by 30° around two neighboring proline residues, Pro^{170} and Pro^{171}, near the C-terminal end of the helix. Furthermore, additional residues near the Pro residues are involved in accommodating the perturbation of the helix by these imino acids. The short nature of this helix results from the presence of the plug, which edges up close to the chromophore. The plug also includes a disulfide bond formed by Cys^{110} and Cys^{187}. From helix IV, Cys^{167} participates in the binding pocket of the chromophore. This helix is tightly coupled through ionic/hydrogen bond interactions with helix II (Tyr^{74}-Glu^{150}, Asn^{78}-Thr^{160}, Asn^{78}-Trp^{161}), interacts through hydrophobic interactions with helix III, and has an additional contact site with helix V (Ala^{166}-Tyr^{206}) (Figure 4; Figure 6*A*, see Suppl. Figure). Interestingly, the disulfide bond formed between Cys^{110} and Cys^{185} cannot substitute for the correct disulfide Cys^{110}-Cys^{187} (90,91). It is important to keep in mind that the Cys^{110}-Cys^{187} bridge is not absolutely essential for retinal-binding because Ala mutants form visual pigments, although with modified bleaching properties (92).

Helix V, formed by residues 200–225 and having a length of 36 Å, is highly tilted by ~26° from the vector perpendicular to the plane of the membrane, and is bent by 25° and 15° at Phe^{203} and His^{211}, respectively, surrounded by aromatic residues at the bends. The bend at His^{211} is caused by Pro^{215}. Helix V forms ionic/hydrogen bond interactions with helix III (Cys^{140}-Thr^{229}, Glu^{122}-Trp^{126}-His^{211}-Tyr^{206} network clustered about a cation or water molecule), helix IV (Ala^{166}-Tyr^{206}), and through hydrophobic interaction with helix VI (Figure 4; Figure 6*A*, see Suppl. Figure). At the cytoplasmic end, helix V breaks around Leu^{226}, followed by a polypeptide chain connecting helix V and VI. This loop is critical in the binding of transducin, arrestin and rhodopsin kinase. Furthermore, this helix provides residues for the binding site for the β-ionone ring of the chromophore (Met^{207}, His^{211}, and Phe^{212}).

Helix VI, the second longest helix in rhodopsin, is composed of residues 244 to 276, 47 Å in length, and only slightly tilted by ~5° from the vector perpendicular to the plane of membranes. It is strongly bent by 30° by Pro^{267}. Helix VI appears to be most loosely associated with other helices in rhodopsin, a feature that could be very important during the activation process. Helix VI interacts through ionic/hydrogen bond interactions with helix III (Arg^{135}-Glu^{247}, important DRY region) and helix VII (Cys^{264}-Thr^{297}) (Figure 4; Figure 6*A*, see Suppl. Figure). Arg^{135} forms a salt bridge with the previous residue, Glu^{134}, but is also connected to Glu^{247} and Thr^{251} in helix VI. These interactions could be critical constraints in keeping rhodopsin in its inactive conformation. Interaction of helix VI with other helices is discussed further below. Hydrophobic residues from this helix (Val^{250}, Met^{253}) form a hydrophobic pocket for the ionic interaction within the DRY region. At the extracellular end of helix VI, Lys^{245}, Lys^{248}, and Arg^{252} form a positively charged cluster, whereas Tyr^{268}, Phe^{261}, Trp^{265}, and Ala^{269} surround the β-ionone ring. Lys^{245} and Lys^{248} residues are 4 and 6 Å, respectively, from the inner limit of the transmembrane domain. The indole ring of Trp^{265} is very close to the β-ionone ring and the C_{13}-methyl group of the chromophore.

Helix VII is critical for rhodopsin function because it contains Lys^{296}, which forms the retinylidene linkage with the chromophore within the transmembrane region. Helix VII is comprised of residues 286–309 and forms a 37 Å-long helix that is minimally tilted with respect to the plane of the membrane (9°), and is significantly bent by 24° and 21° to accommodate linkage with the chromophore around $Pro^{291}$and Pro^{303}. It interacts with helix I (Tyr^{43}-Phe^{293}, Asn^{55}-Ala^{299}), helix III [Glu^{113}-Lys^{296} (retinal)], and helix VI (Cys^{264}-Thr^{297}) through ionic and hydrogen bonds, as well as hydrophobic interactions, and with helix II via

hydrophobic interactions (Figure 4; Figure 6*A*, see Suppl. Figure). Helix VII also stabilizes cytoplasmic helix VIII (Ile^{307}-Arg^{314}) and provides residues that surround the protonated Schiff base. The C-terminal end of this helix contains a highly conserved NPXXY motif in GPCRs. The side chain of a polar residue in the NPXXY region, Asn^{302}, projects toward Asp^{83}. The interaction between these residues may involve water molecules (93). Tyr^{306} also projects inside the rhodopsin molecule and interacts with the conserved Asn^{73} of helix II. In addition, there is a hydrophobic interaction between helices VII and I through Phe^{293} (helix VII) and Leu^{40} (helix I). Residues Lys^{296}-Ala^{299} form a helix in the 3_{10} conformation (three residues per helical turn, and ten atoms in the ring closed by the hydrogen bond). All other helices in rhodopsin are regular α-helices. An additional kink in helix VII is at Val^{300}. This distinct part of the helix (one helical turn) gives more freedom to Lys^{296} because this residue has to accommodate big changes in retinal's structure during the first stages of isomerization. This accommodation greatly decreases the energy barrier of isomerization.

The crystal structure of rhodopsin also revealed one cytoplasmic α-helix. Helix VIII, residues from 311 to 323, spans 16 Å, and forms a straight, short amphiphilic helix connected through ionic/hydrogen bond interactions with helix I (Gln^{64}-Thr^{320}) and helix VII (Ile^{307}-Arg^{314}) (Figure 4; Figure 6*A*, see Suppl. Figure). Elongation of the cytoplasmic surface by helix VIII may allow docking of the transducin Gt trimer (α-, β-, γ-subunits) on the surface of a single photoactivated rhodopsin (94). The C-terminal end of this protein contains Cys^{322} and Cys^{323} with the attached palmitoyl moieties (Figure 3). The presence of these palmitoyl groups, attached enzymatically or spontaneously (46,95), and the loop between helix VII and VIII may affect rhodopsin regeneration (72,96). In COS cells, Cys^{322} and Cys^{323} mutants showed properties similar to those of wild-type rhodopsin (97). It has been proposed that this region of helix VIII and palmitoylation is the site of non-covalent binding of all-*trans*-retinal to opsin (98), in agreement with rhodopsin modeling (D.C. Teller, unpublished data).

Human Diseases Associated with Mutation in the Rhodopsin Gene

Mutations in the rhodopsin gene, mostly missense mutations and some frame-shift mutations, correlate with the autosomal-dominant form of the blinding disease termed retinitis pigmentosa (RP) and account for ~30–40% of all cases of this disease (99,100). The most relevant mutation is Pro^{23}His, which accounts for about 10% of autosomal-dominant RP, but ~100 other mutations were identified throughout rhodopsin. The sites of mutation were previously presented in a two-dimensional model of rhodopsin (34). A null mutation in the rhodopsin gene produces the recessive phenotype, but even heterozygotes have impaired rod vision (101, 102), suggesting the importance of a proper dosage of rhodopsin expression for healthy rod cells. These results are in an agreement with data obtained from rhodopsin knockout mice (103-105). Mice lacking rhodopsin expression do not develop ROS, suggesting that it is also a structural protein necessary for the proper formation of ROS in addition to being a receptor. Many mouse models generated in recent years allow an understanding of how mutations in rhodopsin cause the defect in rod cell biology.

Using the heterologous expression system, these mutants can be classified into three classes: Class I is defective in photoactivation rearrangements, class II remains in the endoplasmic reticulum and does not bind the chromophore, and class III is expressed at low levels and poorly binds chromophore, suggesting a problem with folding and stability (82,106,107). Here, we analyze some of these mutants considering the crystal structure of rhodopsin. Mutations in rhodopsin's extracelullar domain interfere with formation of the plug, destabilizing proper folding of rhodopsin and binding of the chromophore. The C-terminal mutations are most likely associated with the breakdown of vectorial transport to rod outer segments (82). Owing to massive amounts of produced protein, inhibition of this process would lead to blocking the inner segment as a consequence of inefficient disposal of mutated opsin. Mutations in the

transmembrane region of rhodopsin may also lead to constitutive activity (108), metabolically overwhelming the rod photoreceptor cells. Most of these mutations are centered on the chromophore-binding site and intense intramolecular stabilizing interactions are involved (Figure 6*B*, see Suppl. Figure). However, there are also mutations at the lipid-facing residues that most likely prevent proper packing of rhodopsin in ROS disks and/or formation of the organized structure of this protein within the disk.

Chromophore-Binding Site

The retinylidene-binding site is largely hydrophobic, but several charged residues are also present around the chromophore and are necessary for the proper functioning of rhodopsin. The chromophore of rhodopsin, 11-*cis*-retinal, is linked to opsin through a Schiff base (Figure 5). There is clear electron density from the crystal structure analysis that corresponds to the Schiff base and the β-ionone portion of the chromophore (27). The helical nature of the transmembrane segment in the vicinity of Lys^{296} is greatly distorted by Pro^{291} and Pro^{303}. Lys^{296} is located just below the NPXXY region, which forms the C-terminal region of helix VII. The chromophore is in a twisted 6-s-*cis*-conformation within the binding pocket of rhodopsin (Figure 5). The torsion angles for the chromophore are given in a previous publication (28). The Schiff base linkage is protonated, and the counterion on helix III, Glu^{113}, is 3.26 Å away. The vicinity of the Schiff base is formed by residues from helix II (Phe^{91}, Thr^{94}), helix III (Glu^{113}, Ala^{117}), the loop connecting helices IV and V that forms an antiparallel β-sheet and runs under the chromophore (Ser^{186}, Cys^{187}), and helix VII (Ala^{292}, Phe^{293}, Ala^{295}). The kink in the chromophore at C_{11} (the *cis* conformation) is close to Gly^{114}, Ala^{117}, and Thr^{118} of helix III, and to Cys^{187}, and Gly^{188} in the loop connecting helices IV and V. The β-ionone is surrounded by residues from helix III (Thr^{118}, Gly^{121}, Glu^{122}, Leu^{125}), helix IV (Cys^{167}), helix V (Met^{207}, Phe^{208}, His^{211}, Phe^{212}), and helix VI (Phe^{261}, Trp^{265}, Tyr^{268}, Ala^{269}). Thr^{118}, Gly^{188}, Ile^{189}, Tyr^{191}, Tyr^{268} are critical for the proper conformation around the C_9-methyl of the chromophore. Lack of the C_9 methyl group impedes photoactivation (109). Furthermore, Glu^{122} has been proposed to determine the rate of Meta II decay (110) (Figure 5*B*). Water also plays an important part in the binding site, although its location and role are not fully defined based on the crystallographic studies. The only well-defined water molecule is near the retinal chromophore near C_{13} and is hydrogen-bonded to Glu^{181} and Ser^{186} (28). The localization of the chromophore is in reasonable agreement with the cross-linking studies of retinal analogs and identification of Phe^{115}, Ala^{117}, Glu^{122}, Trp^{126}, Ser^{127}, and Trp^{265} as residues in the binding pocket of the β-ionone ring (111,112)[1].

Over the years, retinoid analogs have provided useful information on various photochemical steps during photoactivation, mapping of the chromophore-binding site, and the conformation of the chromophore within rhodopsin [reviewed in (113)]. Opsin reacts within minutes with 11-*cis*-retinal to form rhodopsin. Similarly, 9-*cis*-retinal (also called isorhodopsin) and 7-*cis*-retinal form visual pigments with λ_{max} at 483 nm (114) and 450 nm (115), respectively. When illuminated, 7-*cis*-, 9-*cis*- and 11-*cis*-rhodopsin converge to the same signaling Meta II intermediate (116,117) with quantum efficiencies one seventh, one third, and equal to that of native rhodopsin, respectively. Double and triple *cis*-retinals and a number of analogs are known to reconstitute with opsin. Conversely, all-*trans*-retinal and 13-*cis*-retinal do not regenerate the visual pigment. For rhodopsin, it is generally accepted that 11-*cis*-retinal keeps this receptor in an inactive conformation. The mechanism of these structural constraints imposed by 11-*cis*-retinal may involve multiple hydrophobic and ionic interactions, as described above, that bring helices together, sequester Arg^{135} from the DRY region in a hydrophobic environment, and tighten up the interaction between helices VII and VIII. Light induces the *cis*-*trans* isomerization and rhodopsin activation. However, the active site contains

[1] Cα of Phe^{115} is 6.7 Å from C_{11} of retinal, Phe^{115} (ring center) is 10.0 Å from C_{11} retinal, Trp^{126} (closest atom from ring) is 8.8 Å from C_3 of retinal, and Ser^{127} is 12.

sufficient plasticity to accommodate 7-*cis*- and 9-*cis*-retinal and multiple double *cis*-isomers. This fact suggests either that each of these retinoids induces a different conformation of the protein or that the active site has sufficient fluidity to allow isomers to fit identical or similar binding sites. From the crystal structure of rhodopsin, it appears that the binding site has well-defined binding properties. One involves the fixed position of the Schiff base and the second, the binding of β-ionone in the active site. These two constraints on the chromophore determine the length of the chromophore that will fit into the binding site; any shortening or extending of the chromophore through addition or removal of carbon atoms is non-productive and does not lead to pigment formation (118). Furthermore, rhodopsin regenerated with a retinal with the 11-*cis*-bond constrained by cyclohexanen (6-lock-retinal) or cycloheptanen rings undergoes photoisomerization around other double bonds; however, rhodopsin remains marginally active (119; K. Palczewski, unpublished data). We believe that the isomerization occurs without the chromophore-induced conformational change of the opsin moiety because the β-ionone ring rotates but is largely confined within the binding site of the natural 11-*cis*-retinal chromophore. Isomerization of 6-lock-rhodopsin opens up the chromophore-binding site to nucleophiles, leading to hydrolysis of the chromophore (120,121). Mutation of Trp^{265} to a smaller Phe and regeneration with the six-membered ring of 11-*cis*-retinal leads to formation of truly photostable rhodopsin (122). Whether isomerization of the chromophore is still taking place when bound to the mutant has not been explored. The covalent linkage of the chromophore to opsin is not necessary for the characteristic visible spectrum of rhodopsin or for photoactivation of rhodopsin, as has been elegantly shown using opsin mutants and diffusible 11-*cis*-retinylidene alkylamine analogs (123).

Structural Constraints and Functional Regions

The protein structure must impose the stringent properties that are required for rhodopsin to be a single-photon detector. In a milieu of 10^8 rhodopsin molecules, detection of a single photon requires that noise from all other non-photoactivated rhodopsin be exceedingly low. Therefore, the rhodopsin structure evolved to fulfill this requirement with multiple structural constraints. (*a*) The extracellular plug is highly structured with multiple intradomain interactions fixed by seven transmembrane helices that likely will not allow significant spontaneous conformational changes within this region to take place in the dark or during activation. However, it was noted by others that Cys^{185} is labeled only upon illumination (91,124), suggesting that some conformational changes are possible. This domain is further stabilized by a disulfide bond within this plug (48,90,92,125). (*b*) The chromophore tightens up the structure through multiple hydrophobic interactions, as well as ionic interactions between the protonated Schiff base (helix VII) and its counterion, Glu^{113} (helix III). Mutation of Lys^{296} or Glu^{113} results in opsins that display constitutive activity toward transducin in accordance with the idea that opsin is constrained in an inactive conformation by a salt bridge between Lys^{296} and Glu^{113} (108). (*c*) Asp^{83}, with other residues and in addition to hydrophobic interactions that involve neighboring residues, forms a tight network of interhelical interactions with helix I (Asn^{55} in helix I) and helix VII in the NPXXY region (Asn^{302} via a putative water molecule). (*d*) Highly tilted and central to the bundle of helices, the long helix III interacts with most of the other helices (with the exception of helix I, which is a tightly paired with helix II), especially with helix V (Trp^{126}-His^{211}, Cys^{140}-Thr^{229}, Glu^{122}-Trp^{126}-His^{211}-Tyr^{206}). (*e*) Sequestered Arg^{135} within the hydrophobic pocket is stabilized by ionic interaction with Glu^{134} (the same helix III) and Glu^{247} (helix VI), and further changes the Glu^{225} and Tyr^{136} hydrogen bonding (Figure 6*A*). It appears that Arg^{135} is critical for the interaction of photoactivated rhodopsin with transducin (126,127); therefore, sequestering these residues may eliminate one of the key interactions between these two proteins. Arg^{135} is highly conserved among GPCRs in the so-called DRY motif. (*f*) The NPXXY region interacts with the double-palmitoylated helix VIII and brings it close to the rest of the protein. The movement of helix VIII is observed during rhodopsin activation (128) (Figure 6*B*). Furthermore, an anti-Meta II antibody that recognizes

residues 304–311 (a hinge between helix VII and helix VIII) does not react with rhodopsin or opsin (129).

Previous Models: Prediction, Bacteriorhodopsin and Cryo-Electron Microscopy

For years, the rhodopsin structure has been compared with that of bacteriorhodopsin, also a retinylidene seven-transmembrane protein. However, the arrangements of the seven helices were found to be different on the basis of earlier low-resolution studies on rhodopsin using cryo-electron microscopy at 7.5 Å resolution in the plane of the membrane and at 16.5 Å resolution perpendicular to the membrane (130-132) [see structural comparison in (28)]. The projection map of invertebrate rhodopsin is also similar to maps previously determined for bovine and frog rhodopsins (133). In rhodopsin, the helices are slightly longer than those of bacteriorhodopsin and differently arranged. Helices IV and V of the two proteins do not superimpose (whereas helices I, II, and III are similar). The helices in rhodopsin are more tilted and kinked, and its extramembrane regions are larger and more organized. Rhodopsin also contains an extra helix (helix VIII). The retinal chromophore is in the twisted 6-s-*cis* conformation in rhodopsin, whereas in bacteriorhodopsin it is 6-s-*trans*-conformation. In addition, the retinylidene groups in the two proteins are in different positions relative to the membrane plane, although the ionone rings are placed in similar positions. Because G protein receptors were not amenable for crystallographic studies, three-dimensional models based on the modeling studies were proposed. A particular model of rhodopsin was computed that closely resembles the transmembrane region structure found from the actual crystal structure (134). Similar models were also generated for other GPCRs (135).

A superimposition of the crystal structure of bovine rhodopsin and a model of frog rhodopsin from cryo-electron microscopy (gray balls), obtained under different resolutions and in different packing environments, are generally in agreement (Figure 7, see Supplemental Materials: Follow the Supplemental Material link on the Annual Reviews homepage at http://annualreviews.org/). However, the largest differences are seen within helices I, III, and VII. Remarkably, several of the kinked helices are observed in both structures. In addition to these structural studies, UV, FTIR, NMR, and EPR spectroscopic investigations of rhodopsin and its mutants in inactive and photoactivated states provide additional validation of the crystallographic model and further significant insights into rhodopsin structure and activation. Owing to space limitation, these spectroscopic studies cannot be fully evaluated herein.

ACTIVATION MECHANISM OF RHODOPSIN

Unified Model

Although the activation of rhodopsin is still roughly sketched, the crystal structure of rhodopsin provides the opportunity to summarize our current understanding of this process. The present view is inevitably oversimplified because of a vast amount of information existing in the literature. Therefore, the objective is to present a simplified, but coherent, hypothesis that unites major findings on rhodopsin activation. The reader should also consult recent publications (34,75,136,137). One should also reflect on the complexity of the interactions with the transmembrane segment of rhodopsin (Figure 6*A*, see Suppl. Figure). Our activation model discusses only the major determinants of the activation process.

A photon of visible light absorbed by rhodopsin provides sufficient energy for the structural transformation from quiescence into a signaling protein. First, photoisomerization causes transformation of 11-*cis*-retinylidene to all-*trans*-retinylidene. The quantum yield for this reaction is ~0.67 (138). The reaction is too fast for any significant conformational change in opsin (139) (Figure 8, see Supplemental Materials: Follow the Supplemental Material link on the Annual Reviews homepage at http://annualreviews.org/). Twisting of all-*trans*-retinylidene

within the original 11-*cis*-retinylidene binding site of opsin is a way by which two thirds of the 55 kcal/mol energy of the photon is stored in the all-*trans*-retinylidene-opsin complex (140). This energy is then released during relaxation of earlier intermediates to the signaling stage of the receptor, Meta II. Formation of Meta II leads to relocation of the β-ionone ring to a new position, as proposed by cross-linking studies (141)[2] (Figure 8, see Suppl. Figure). Photoisomerization of the chromophore may initially involve reorganization of the 3_{10} helical region of helix VII. The consequence of this movement is the breakage of a salt bridge between Glu^{113} and the protonated Schiff base between Lys^{296} and the retinal (108). This involves movement of a proton from the donor to the acceptor (142) in conjunction with the motion of the transmembrane helices (136,143). The movement of helix VII away from helix I by 2–4 Å and the pushing of helix VI (64) ~3 Å by the photolyzed chromophore from the first cytoplasmic loop lead to removal of Glu^{247} from the ionic interaction in the DRY region (Figure 6) [summarized in (136)]. Subsequent movement of Arg^{135} to the cytosol allows photoactivated rhodopsin to attract and interact with transducin. Protonation of Glu^{134}, which is left in a very hydrophobic milieu, completes this transformation (34). This would reflect changes attributed to the central helix III (144). It is also important to note that helix VI is only loosely associated with the remaining bundle of helices (28) (Figures 4 and 7). The residues in helix VI, particularly Pro^{267}, affect the assembly of rhodopsin from two fragments and the conformation of the cytoplasmic loop III (72). For the α_{1B}-adrenergic receptor, this region has been identified as key to the coupling process with its G protein (145). Therefore, the charge-neutralizing mutation Glu^{134} to Gln^{134} produces hyperactivity in the activated state and produces constitutive activity in opsin (144). The consequences of photoactivation are also transmitted toward a second region, the NPXXY cluster in helix VII. Structural changes connected with activation have been detected using spin labels at residues 306, 313, and 316. The changes at side-chain 313 can be accounted for by movements in the adjacent helix VII (146). Movement of this helix is critical for efficient coupling with transducin (147,148). Methyl groups, in particular the C_9-methyl group on retinal, are critical for efficient movement of this helix (O.P. Ernst, K.P. Hofmann & K. Palczewski, unpublished data). The separation of helices on the cytoplasmic side of Meta II opens up a cavity into which transducin can dock (149). The formation of Meta II is transiently stabilized by rearrangement of the Glu^{122}-Trp^{126}-His^{211} triad (helices III–V) (150) before Meta II decays to opsin. Therefore, the activation process could be considered a removal of structural constraints in rhodopsin, and it is not surprising that a soluble cytoplasmic domain grafted into soluble proteins is very effective in the stimulation of transducin (151). It is important to note that certain phospholipids may impede these conformational changes (152).

Cavities and the Second Chromophore-Binding Site

The resolution of the rhodopsin structure is 2.8 Å and does not allow precise localization of all water molecules associated with the receptor. We have identified several regions around the chromophore and intracellular face that could be occupied by water molecules in the dark state, as well as large cavities suitable for protein-protein interactions (Figure 9, see Supplemental Materials: Follow the Supplemental Material link on the Annual Reviews homepage at http://annualreviews.org/). Water molecules could be involved in the activation process similar to the role of water in the bacteriorhodopsin photocycle. The reorganization of water molecules during activation has been detected by FTIR spectroscopy (153). Furthermore, one of these cavities could be involved in the non-covalent binding of all-*trans*-retinal, which activates opsin in transducin, arrestin, and rhodopsin kinase assays [reviewed in (60)]. One such binding site may be present around helix VIII and the palmitoylation sites (D.C. Teller, unpublished data). A recent refinement of rhodopsin at 2.6 Å resolution has provided an updated view of the contributions of water molecules to the activity of the protein (93).

[2]Agreement with cross-linking studies with the crystal structure of rhodopsin requires that during the photoactivating process, helix IV undergoes a large rotation. Indep

CONE VISUAL PIGMENTS

Although a full analysis of spectral tuning and the properties of the cone pigments is outside the scope of this review, a few points are worth mentioning. Rhodopsin appears to be an ideal structural template for cone pigments. We carried out homology modeling for cone pigments that revealed several interesting features related to the DRY region (Figure 8*A*) and the chromophore-binding sites (Figure 8*B*) (154). In contrast, the NPXXY region is highly homologous among cone pigments and rhodopsin (data not shown). The only difference in the chromophore-binding site between green and red pigments is in the immediate vicinity of retinal, where Phe^{261} is replaced by Tyr^{261} (red), as predicted from studies on the spectral tuning of primates aimed at understanding the molecular properties underlying red-green color vision (155, 156). These studies were extended to identify residues responsible in in vitro experiments [157, 158; reviewed in (159)]. Furthermore, it has been convincingly documented that these in vitro analyses correlate with the in vivo data based on psychophysical measurements (160). The difference in λ_{max} between the green and red pigments has been proposed to result from other hydroxyl-bearing amino acids (Ser^{164} and Thr^{269}) that are farther away from the chromophore [(161); reviewed in (159)]. These earlier findings were confirmed by more recent studies (162). The difference between rhodopsin and green pigments (30 nm blue shift) could be accounted for by the increased hydrogen bonding of the protonated Schiff base group in rhodopsin (163). In the chromophore-binding site, Ser^{202} is shown to hydrogen bond with Glu^{113} in the blue pigment, but points toward a Cl^- ion in the red/green pigment. Through mutagenesis studies, two residues, His^{197} and Lys^{200}, were identified in the Cl^--binding site of red and green visual pigments (79). In our model, Lys^{200} does not participate in the binding of this ion.

OTHER G PROTEIN-COUPLED RECEPTORS

An enormous set of information must flow across the cell surface to the cell to ensure survival, and transmembrane proteins play a key role in this process. Membrane proteins, among them rhodopsin-like proteins, GPCRs, represent a large and versatile group of protein sensors involved in nearly all physiological processes in vertebrates. In all organisms, from the most primitive to mammals, but perhaps not in plants, GPCRs are present in multiple molecular forms. For example, 5–10% of the *Homo sapiens* genome encodes GPCRs, which translates into >600 non-sensory and 1000s of sensory GPCRs. These molecules are involved in decoding information through the olfaction, vision, and taste systems, and comprise one of the largest families of proteins encoded by our genome. Understanding how rhodopsin, the best-studied member of this family, works reaches far beyond its key role in vision. Parallel information that can be learned from phototransduction is directly implemented into a better picture of other signal transduction via GPCRs, one of the most important topics in current neurobiology/pharmacology.

GPCRs transduce an extracellular signal by coupling with G proteins on the cytoplasmic side of the cell; the binding site for the activating ligand is either within the hydrophobic bundle of helices or at an extracellular domain of these receptors. There is a growing body of evidence that these receptors may also modulate the intracellular processes independently of G proteins (164). On the basis of the conservation pattern of the primary amino acid sequence, three major families of GPCRs have been described (165). Family 1 (or A), the largest of the three, is defined by receptors whose sequences are homologous to rhodopsin, including opiate, adrenergic, cannabinoid, and muscarinic receptors. Family 2 (or B) consists of GPCRs homologous in sequence to the secretin receptor, and Family 3 (or C) includes GPCRs homologous in sequence to the GABA receptor. The overall homology between receptors even within the same family is low (frequently <35%). However, some regions are highly conserved, suggesting that their function is either structural or related to the molecular mechanism of

receptor activation. Some of these conserved residues, clustered in space, define conserved three-dimensional motifs referred to as functional microdomains (167,169). The functional microdomains include the DRY region (Figure 9*B*, in rhodopsin ERY), helix VIII and palmitoyl moieties, the NPXXY region, a ligand-binding site, a Pro kink in helix VI, a disulfide bond, and oligosaccharide moieties. Therefore, rhodopsin is a very useful template for all GPCRs, at least until more high-resolution structures become available, especially for Family 1 (163).

The structure and organization of rhodopsin and other GPCRs in native membranes is not known. For many GPCRs, including adenosine, adrenergic, dopamine, opioid, and other receptors, dimeric structures have been more or less stringently documented (166).

FINAL REMARKS

In coming years, further advances will be made by understanding all of the proteins and complexes in different signaling states on a structural level and by giving reliable and logical chemical/physical models of visual transduction at an atomic resolution that will be coherent and consistent with thermodynamic laws. The structures of G proteins, arrestins, and now rhodopsin are the first steps toward these goals. Similar to research on the metabolic pathways in the past 10–20 years, signal transduction by GPCRs has become a very mature field. However, many fundamental questions remain in relation to the activation mechanism of GPCRs, the specificity and recognition of interacting proteins and their mechanisms of activation by GPCRs, and the structure of receptors and interacting proteins in the native setting of phospholipids in in vivo conditions. The great interest in these topics from academic and industrial laboratories makes it certain that further progress will be made.

ACKNOWLEDGMENTS

We thank Yunie Kim for her outstanding help during manuscript preparation. This research was supported in part by U.S. Public Health Service grants EY01730, EY08061 and EY0861; from the National Eye Institute, National Institutes of Health, grant GM63020; an unrestricted grant from Research to Prevent Blindness, Inc. (RPB) to the Department of Ophthalmology at the University of Washington; and a grant from the E.K. Bishop Foundation. Calculations and visualizations were partly done in the ICM Computer Center, University of Warsaw, Poland.

LITERATURE CITED

1. Kühne, W. Ueber den Sehpurpur. Unters. Physiol. Inst. Univ. Heidelberg; Heidelberg: 1878. p. 113
2. Wald G. Carotenoids and the visual cycle. J. Gen. Physiol 1935–1936;19:351–71.
3. Hubbard R, Kropf A. Molecular isomers in vision. Sci. Am 1967;216:64–70. [PubMed: 6046324]
4. Wald G. The molecular basis of visual excitation. Nature 1968;219:800–7. [PubMed: 4876934]
5. Matthews RG, Hubbard R, Brown PK, Wald G. Tautomeric forms of meta-rhodopsin. J. Gen. Physiol 1963;47:215–40. [PubMed: 14080814]
6. Hargrave PA. Rhodopsin chemistry, structure and topography. Prog. Retinal Res 1982;1:1–51.
7. Hargrave PA, McDowell JH, Curtis DR, Wang JK, Juszczak E, et al. The structure of bovine rhodopsin. Biophys. Struct. Mech 1983;9:235–44. [PubMed: 6342691]
8. Ovchinnikov YA. Rhodopsin and bacteriorhodopsin: structure-function relationships. FEBS Lett 1982;148:179–91. [PubMed: 6759163]
9. Argos P, Rao JK, Hargrave PA. Structural prediction of membrane-bound proteins. Eur. J. Biochem 1982;128:565–75. [PubMed: 7151796]
10. Fung BK-K, Stryer L. Photolyzed rhodopsin catalyzes the exchange of GTP for bound GDP in retinal. Proc. Natl. Acad. Sci. USA 1980;77:2500–4. [PubMed: 6930647]
11. Kuhn H, Bennett N, Michel Villaz M, Chabre M. Interactions between photoexcited rhodopsin and GTP-binding protein. Proc. Natl. Acad. Sci. USA 1981;78:6873–77. [PubMed: 6273893]
12. Longstaff C, Calhoon RD, Rando RR. Deprotonation of the Schiff base of rhodopsin is obligate in the activation of the G protein. Proc. Natl. Acad. Sci. USA 1986;83:4209–13. [PubMed: 3012559]

13. Bownds D, Dawes J, Miller J, Stahlman M. Phosphorylation of frog photoreceptor membranes induced by light. Nat. New Biol 1972;237:125–27. [PubMed: 4503852]
14. Frank RN, Cavanagh HD, Kenyon KR. Light-stimulated phosphorylation of bovine visual pigments by adenosine triphosphate. J. Biol. Chem 1973;248:596–609. [PubMed: 4346338]
15. Kuhn H, Dreyer WJ. Light dependent phosphorylation of rhodopsin by ATP. FEBS Lett 1972;20:1–6. [PubMed: 11946367]
16. Liebman PA, Pugh EN Jr. ATP mediates rapid reversal of cyclic GMP phosphodiesterase activation in visual receptor membranes. Nature 1980287:734–36. [PubMed: 6107856]
17. Sitaramayya A, Liebman PA. Phosphorylation of rhodopsin and quenching of cyclic GMP phosphodiesterase activation by ATP at weak bleaches. J. Biol. Chem 1983;258:12106–9. [PubMed: 6313637]
18. Palczewski K, McDowell JH, Hargrave PA. Purification and characterization of rhodopsin kinase. J. Biol. Chem 1988;263:14067–73. [PubMed: 2844754]
19. Lorenz W, Inglese J, Palczewski K, Onorato JJ, Caron MG, Lefkowitz RJ. The receptor kinase family: Primary structure of rhodopsin kinase reveals similarities to the beta-adrenergic receptor kinase. Proc. Natl. Acad. Sci. USA 1991;88:8715–19. [PubMed: 1656454]
20. Wilden U, Hall SW, Kuhn H. Phosphodiesterase activation by photoexcited rhodopsin is quenched when rhodopsin is phosphorylated and binds the intrinsic 48-kDa protein of rod outer segments. Proc. Natl. Acad. Sci. USA 1986;83:1174–78. [PubMed: 3006038]
21. Palczewski K. Structure and functions of arrestins. Protein Sci 1994;3:1355–61. [PubMed: 7833798]
22. Nathans J, Hogness DS. Isolation, sequence analysis, and intron-exon arrangement of the gene encoding bovine rhodopsin. Cell 1983;34:807–14. [PubMed: 6194890]
23. Nathans J, Hogness DS. Isolation and nucleotide sequence of the gene encoding human rhodopsin. Proc. Natl. Acad. Sci. USA 1984;81:4851–55. [PubMed: 6589631]
24. Nathans J, Thomas D, Hogness DS. Molecular genetics of human color vision: the genes encoding blue, green, and red pigments. Science 1986;232:193–202. [PubMed: 2937147]
25. Zuker CS, Cowman AF, Rubin GM. Isolation and structure of a rhodopsin gene from *D. melanogaster*. Cell 1985;40:851–58. [PubMed: 2580638]
26. Ferretti L, Karnik SS, Khorana HG, Nassal M, Oprian DD. Total synthesis of a gene for bovine rhodopsin. Proc. Natl. Acad. Sci. USA 1986;83:599–603. [PubMed: 3456156]
27. Palczewski K, Kumasaka T, Hori T, Behnke CA, Motoshima H, et al. Crystal structure of rhodopsin: a G protein-coupled receptor. Science 2000;289:739–45. [PubMed: 10926528]
28. Teller DC, Okada T, Behnke CA, Palczewski K, Stenkamp RE. Advances in determination of a high-resolution three-dimensional structure of rhodopsin, a model of G-protein-coupled receptors (GPCRs). Biochemistry 2001;40:7761–72. [PubMed: 11425302]
29. Ebrey T, Koutalos Y. Vertebrate photoreceptors. Prog. Retina Eye Res 2001;20:49–94.
30. Fain GL, Matthews HR, Cornwall MC, Koutalos Y. Adaptation in vertebrate photoreceptors. Physiol. Rev 2001;81:117–51. [PubMed: 11152756]
31. Polans A, Baehr W, Palczewski K. Turned on by Ca^{2+}! The physiology and pathology of Ca^{2+}-binding proteins in the retina. Trends Neurosci 1996;19:547–54. [PubMed: 8961484]
32. Khorana HG. Molecular biology of light transduction by the mammalian photoreceptor, rhodopsin. J. Biomol. Struct. Des 1999;1:1–16.
33. Menon ST, Han M, Sakmar TP. Rhodopsin: structural basis of molecular physiology. Physiol. Rev 2001;81:1659–88. [PubMed: 11581499]
34. Okada T, Ernst OP, Palczewski K, Hofmann KP. Activation of rhodopsin: new insights from structural and biochemical studies. Trends Biochem. Sci 2001;26:318–24. [PubMed: 11343925]
35. Palczewski K, Benovic JL. G-protein-coupled receptor kinases. Trends Biochem. Sci 1991;16:387–91. [PubMed: 1664548]
36. Palczewski K, Polans AS, Baehr W, Ames JB. Ca^{2+}-binding proteins in the retina: structure, function, and the etiology of human visual diseases. BioEssays 2000;22:337–50. [PubMed: 10723031]
37. Zhao X, Yokoyama K, Whitten ME, Huang J, Gelb MH, Palczewski K. A novel form of rhodopsin kinase from chicken retina and pineal gland. FEBS Lett 1999;454:115–21. [PubMed: 10413107]

38. Treisman JE, Morabito MA, Barnstable CJ. Opsin expression in the rat retina is developmentally regulated by transcriptional activation. Mol. Cell. Biol 1988;8:1570–79. [PubMed: 2967911]
39. Litman BJ. Purification of rhodopsin by concanavalin A affinity chromatography. Methods Enzymol 1982;81:150–53. [PubMed: 7098858]
40. Hong K, Knudsen PJ, Hubbell WL. Purification of rhodopsin on hydroxyapatite columns, detergent exchange, and recombination with phospholipids. Methods Enzymol 1982;81:144–50. [PubMed: 6285125]
41. Oprian DD, Asenjo AB, Lee N, Pelletier SL. Design, chemical synthesis, and expression of genes for the three human color vision pigments. Biochemistry 1991;30:11367–72. [PubMed: 1742276]
42. Deleted in proof
43. Okada T, Le Trong I, Fox BA, Behnke CA, Stenkamp RE, Palczewski K. X-ray diffraction analysis of three-dimensional crystals of bovine rhodopsin obtained from mixed micelles. J. Struct. Biol 2000;130:73–80. [PubMed: 10806093]
44. Bownds D. Site of attachment of retinal in rhodopsin. Nature 1967;216:1178–81. [PubMed: 4294735]
45. Hargrave PA, Fong SL. The amino-and carboxyl-terminal sequence of bovine rhodopsin. J. Supramol. Struct 1977;6:559–70. [PubMed: 592823]
46. O'Brien PJ, Zatz M. Acylation of bovine rhodopsin by [^{3}H]palmitic acid. J. Biol. Chem 1984;259:5054–57. [PubMed: 6715336]
47. Ovchinnikov YA, Abdulaev NG, Bogachuk AS. Two adjacent cysteine residues in the C-terminal cytoplasmic fragment of bovine rhodopsin are palmitylated. FEBS Lett 1988;230:1–5. [PubMed: 3350146]
48. Karnik SS, Sakmar TP, Chen HB, Khorana HG. Cysteine residues 110 and 187 are essential for the formation of correct structure in bovine rhodopsin. Proc. Natl. Acad. Sci. USA 1988;85:8459–63. [PubMed: 3186735]
49. Fukuda MN, Papermaster DS, Hargrave PA. Structural analysis of carbohydrate moiety of bovine rhodopsin. Methods Enzymol 1982;81:214–23. [PubMed: 7098866]
50. Schey KL, Papac DI, Knapp DR, Crouch RK. Matrix-assisted laser desorption mass spectrometry of rhodopsin and bacteriorhodopsin. Biophys. J 1992;63:1240–43. [PubMed: 1477275]
51. Palczewski K, Buczylko J, Kaplan MW, Polans AS, Crabb JW. Mechanism of rhodopsin kinase activation. J. Biol. Chem 1991;266:12949–55. [PubMed: 2071581]
52. Ohguro H, Rudnicka-Nawrot M, Buczylko J, Zhao X, Taylor JA, et al. Structural and enzymatic aspects of rhodopsin phosphorylation. J. Biol. Chem 1996;271:5215–24. [PubMed: 8617805]
53. Ohguro H, Van Hooser JP, Milam AH, Palczewski K. Rhodopsin phosphorylation and dephosphorylation in vivo. J. Biol. Chem 1995;270:14259–62. [PubMed: 7782279]
54. Sokal I, Pulvermuller A, Buczylko J, Hofmann KP, Palczewski K. Rhodopsin and its kinase. Methods Enzymol 2002;343:578–600. [PubMed: 11665593]
55. Wang Q, Schoenlein RW, Peteanu LA, Mathies RA, Shank CV. Vibrationally coherent photochemistry in the femtosecond primary event of vision. Science 1994;266:422–24. [PubMed: 7939680]
56. Liu RS. Photoisomerization by hula-twist: a fundamental supramolecular photochemical reaction. Acc. Chem. Res 2001;34:555–62. [PubMed: 11456473]
57. Shichida Y, Imai H. Visual pigment: G-protein-coupled receptor for light signals. Cell. Mol. Life Sci 1998;54:1299–315. [PubMed: 9893707]
58. Janz JM, Farrens DL. Engineering a functional blue-wavelength-shifted rhodopsin mutant. Biochemistry 2001;40:7219–27. [PubMed: 11401569]
59. Szundi I, Mah TL, Lewis JW, Jager S, Ernst OP, et al. Proton transfer reactions linked to rhodopsin activation. Biochemistry 1998;37:14237–44. [PubMed: 9760262]
60. McBee JK, Palczewski K, Baehr W, Pepperberg DR. Confronting complexity: the interlink of phototransduction and retinoid metabolism in the vertebrate retina. Prog. Retin. Eye Res 2001;20:469–529. [PubMed: 11390257]
61. Kefalov VJ, Cornwall MC, Crouch RK. Occupancy of the chromophore binding site of opsin activates visual transduction in rod photoreceptors. J. Gen. Physiol 1999;113:491–503. [PubMed: 10051522]

62. Arnis S, Hofmann KP. Photoregeneration of bovine rhodopsin from its signaling state. Biochemistry 1995;34:9333–40. [PubMed: 7626602]
63. Bartl FJ, Ritter E, Hofmann KP. Signaling states of rhodopsin: absorption of light in active metarhodopsin II generates an all-*trans*-retinal bound inactive state. J. Biol. Chem 2001;276:30161–66. [PubMed: 11384968]
64. Oprian DD, Molday RS, Kaufman RJ, Khorana HG. Expression of a synthetic bovine rhodopsin gene in monkey kidney cells. Proc. Natl. Acad. Sci. USA 1987;84:8874–78. [PubMed: 2962193]
65. Klaassen CH, DeGrip WJ. Baculovirus expression system for expression and characterization of functional recombinant visual pigments. Methods Enzymol 2000;315:12–29. [PubMed: 10736691]
66. Abdulaev NG, Ridge KD. Heterologous expression of bovine opsin in *Pichia pastoris*. Methods Enzymol 2000;315:3–11. [PubMed: 10736690]
67. Mollaaghababa R, Davidson FF, Kaiser C, Khorana HG. Structure and function in rhodopsin: expression of functional mammalian opsin in *Saccharomyces cerevisiae*. Proc. Natl. Acad. Sci. USA 1996;93:11482–86. [PubMed: 8876161]
68. Nathans J. Determinants of visual pigment absorbance: identification of the retinylidene Schiff's base counterion in bovine rhodopsin. Biochemistry 1990;29:9746–52. [PubMed: 1980212]
69. Zhukovsky EA, Oprian DD. Effect of carboxylic acid side chains on the absorption maximum of visual pigments. Science 1989;246:928–30. [PubMed: 2573154]
70. Sakmar TP, Franke RR, Khorana HG. Glutamic acid-113 serves as the retinylidene Schiff base counterion in bovine rhodopsin. Proc. Natl. Acad. Sci. USA 1989;86:8309–13. [PubMed: 2573063]
71. Kaushal S, Ridge KD, Khorana HG. Structure and function in rhodopsin: the role of asparagine-linked glycosylation. Proc. Natl. Acad. Sci. USA 1994;91:4024–28. [PubMed: 8171029]
72. Ridge KD, Ngo T, Lee SS, Abdulaev NG. Folding and assembly in rhodopsin. Effect of mutations in the sixth transmembrane helix on the conformation of the third cytoplasmic loop. J. Biol. Chem 1999;274:21437–42. [PubMed: 10409707]
73. Ridge KD, Lee SS, Yao LL. In vivo assembly of rhodopsin from expressed polypeptide fragments. Proc. Natl. Acad. Sci. USA 1995;92:3204–8. [PubMed: 7724540]
74. Okada T, Takeda K, Kouyama T. Highly selective separation of rhodopsin from bovine rod outer segment membranes using combination of divalent cation and alkyl(thio)glucoside. Photochem. Photobiol 1998;67:495–99. [PubMed: 9613234]
75. Okada T, Palczewski K. Crystal structure of rhodopsin: implications for vision and beyond. Curr. Opin. Struct. Biol 2001;11:420–26. [PubMed: 11495733]
76. Royant A, Nollert P, Edman K, Neutze R, Landau EM, et al. X-ray structure of sensory rhodopsin II at 2.1-Å resolution. Proc. Natl. Acad. Sci. USA 2001;98:10131–36. [PubMed: 11504917]
77. Thomas DD, Stryer L. Transverse location of the retinal chromophore of rhodopsin in rod outer segment disc membranes. J. Mol. Biol 1982;154:145–57. [PubMed: 7077659]
78. Yan EC, Kazmi MA, De S, Chang BS, Seibert C, et al. Function of extracellular loop 2 in rhodopsin: glutamic acid 181 modulates stability and absorption wavelength of metarhodopsin II. Biochemistry 2002;41:3620–27. [PubMed: 11888278]
79. Wang Z, Asenjo AB, Oprian DD. Identification of the Cl(−)-binding site in the human red and green color vision pigments. Biochemistry 1993;32:2125–30. [PubMed: 8443153]
80. Crescitelli, F. Handbook of Sensory Physiology. Springer-Verlag; New York: 1977. The visual pigments of geckos and other vertebrates: an essay in comparative biology; p. 391-449.
81. Moritz OL, Tam BM, Papermaster DS, Nakayama T. A functional rhodopsin-green fluorescent protein fusion protein localizes correctly in transgenic *Xenopus laevis* retinal rods and is expressed in a time-dependent pattern. J. Biol. Chem 2001;276:28242–51. [PubMed: 11350960]
82. Sung CH, Makino C, Baylor D, Nathans J. A rhodopsin gene mutation responsible for autosomal dominant retinitis. J. Neurosci 1994;14:5818–33. [PubMed: 7523628]
83. Tam BM, Moritz OL, Hurd LB, Papermaster DS. Identification of an outer segment targeting signal in the COOH terminus of rhodopsin using transgenic *Xenopus laevis*. J. Cell Biol 2000;151:1369–80. [PubMed: 11134067]

84. Cideciyan AV, Zhao X, Nielsen L, Khani SC, Jacobson SG, Palczewski K. Null mutation in the rhodopsin kinase gene slows recovery kinetics of rod and cone phototransduction in man. Proc. Natl. Acad. Sci. USA 1998;95:328–33. [PubMed: 9419375]

85. Langen R, Cai K, Altenbach C, Khorana HG, Hubbell WL. Structural features of the C-terminal domain of bovine rhodopsin: a site-directed spin-labeling study. Biochemistry 1999;38:7918–24. [PubMed: 10387033]

86. Mielke T, Villa C, Edwards PC, Schertler GF, Heyn MP. X-ray diffraction of heavy-atom labelled two-dimensional crystals of rhodopsin identifies the position of cysteine 140 in helix 3 and cysteine 316 in helix 8. J. Mol. Biol 2002;316:693–709. [PubMed: 11866527]

87. Sipos L, von Heijne G. Predicting the topology of eukaryotic membrane proteins. Eur. J. Biochem 1993;213:1333–40. [PubMed: 8099327]

88. Hartmann E, Rapoport TA, Lodish HF. Predicting the orientation of eukaryotic membrane-spanning proteins. Proc. Natl. Acad. Sci. USA 1989;86:5786–90. [PubMed: 2762295]

89. Popot JL, Engelman DM. Helical membrane protein folding, stability, and evolution. Annu. Rev. Biochem 2000;69:881–922. [PubMed: 10966478]

90. Hwa J, Reeves PJ, Klein-Seetharaman J, Davidson F, Khorana HG. Structure and function in rhodopsin: further elucidation of the role of the intradiscal cysteines, Cys-110, -185, and -187, in rhodopsin folding and function. Proc. Natl. Acad. Sci. USA 1999;96:1932–35. [PubMed: 10051572]

91. Ridge KD, Lu Z, Liu X, Khorana HG. Structure and function in rhodopsin. Separation and characterization of the correctly folded and misfolded opsins produced on expression of an opsin mutant gene containing only the native intradiscal cysteine codons. Biochemistry 1995;34:3261–67. [PubMed: 7880821]

92. Davidson FF, Loewen PC, Khorana HG. Structure and function in rhodopsin: replacement by alanine of cysteine residues 110 and 187, components of a conserved disulfide bond in rhodopsin, affects the light-activated metarhodopsin II state. Proc. Natl. Acad. Sci. USA 1994;91

93. Okada T, Fujiyoshi Y, Silow M, Navarro J, Landau EM, Shichida Y. Functional role of internal water molecules in rhodopsin revealed by X-ray crystallography. Proc. Natl. Acad. Sci. USA 2002;99:5982–87. [PubMed: 11972040]

94. Kisselev OG, Meyer CK, Heck M, Ernst OP, Hofmann KP. Signal transfer from rhodopsin to the G-protein: evidence for a two-site sequential fit mechanism. Proc. Natl. Acad. Sci. USA 1999;96:4898–903. [PubMed: 10220390]

95. Veit M, Sachs K, Heckelmann M, Maretzki D, Hofmann KP, Schmidt MF. Palmitoylation of rhodopsin with S-protein acyltransferase: enzyme catalyzed reaction versus autocatalytic acylation. Biochim. Biophys. Acta 1998;1394:90–98. [PubMed: 9767130]

96. Weiss ER, Osawa S, Shi W, Dickerson CD. Effects of carboxyl-terminal truncation on the stability and G protein-coupling activity of bovine rhodopsin. Biochemistry 1994;33:7587–93. [PubMed: 8011624]

97. Karnik SS, Ridge KD, Bhattacharya S, Khorana HG. Palmitoylation of bovine opsin and its cysteine mutants in COS cells. Proc. Natl. Acad. Sci. USA 1993;90:40–44. [PubMed: 8419942]

98. Sachs K, Maretzki D, Meyer CK, Hofmann KP. Diffusible ligand all-*trans*-retinal activates opsin via a palmitoylation-dependent mechanism. J. Biol. Chem 2000;275:6189–94. [PubMed: 10692411]

99. Rattner A, Sun H, Nathans J. Molecular genetics of human retinal disease. Annu. Rev. Genet 1999;33:89–131M. [PubMed: 10690405]

100. Dryja TP, Li T. Molecular genetics of retinitis pigmentosa. Hum. Mol. Genet 1995;4:1739–43. [PubMed: 8541873]

101. Rosenfeld PJ, Cowley GS, McGee TL, Sandberg MA, Berson EL, Dryja TP. A null mutation in the rhodopsin gene causes rod photoreceptor dysfunction and autosomal recessive retinitis pigmentosa. Nat. Genet 1992;1:209–13. [PubMed: 1303237]

102. Kumaramanickavel G, Maw M, Denton MJ, John S, Srikumari CR, et al. Missense rhodopsin mutation in a family with recessive RP. Nat. Genet 1994;8:10–11. [PubMed: 7987385]

103. Toda K, Bush RA, Humphries P, Sieving PA. The electroretinogram of the rhodopsin knockout mouse. Vis. Neurosci 1999;16:391–98. [PubMed: 10367972]

104. Humphries MM, Rancourt D, Farrar GJ, Kenna P, Hazel M, et al. Retinopathy induced in mice by targeted disruption of the rhodopsin gene. Nat. Genet 1997;15:216–19. [PubMed: 9020854]

105. Lem J, Krasnoperova NV, Calvert PD, Kosaras B, Cameron DA, et al. Morphological, physiological, and biochemical changes in rhodopsin knockout mice. Proc. Natl. Acad. Sci. USA 1999;96:736–41. [PubMed: 9892703]
106. Jacobson SG, Kemp CM, Sung CH, Nathans J. Retinal function and rhodopsin levels in autosomal dominant retinitis. Am. J. Ophthalmol 1991;112:256–71. [PubMed: 1882937]
107. Kaushal S, Khorana HG. Structure and function in rhodopsin. 7. Point mutations associated with autosomal dominant retinitis pigmentosa. Biochemistry 1994;33:6121–28. [PubMed: 8193125]
108. Rao VR, Oprian DD. Activating mutations of rhodopsin and other G protein-coupled receptors. Annu. Rev. Biophys. Biomol. Struct 1996;25:287–314. [PubMed: 8800472]
109. Vogel R, Fan GB, Sheves M, Siebert F. The molecular origin of the inhibition of transducin activation in rhodopsin lacking the 9-methyl group of the retinal chromophore: a UV-Vis and FTIR spectroscopic study. Biochemistry 2000;39:8895–908. [PubMed: 10913302]
110. Imai H, Kojima D, Oura T, Tachibanaki S, Terakita A, Shichida Y. Single amino acid residue as a functional determinant of rod and cone visual pigments. Proc. Natl. Acad. Sci. USA 1997;94:2322–26. [PubMed: 9122193]
111. Nakayama TA, Khorana HG. Mapping of the amino acids in membrane-embedded helices that interact with the retinal chromophore in bovine rhodopsin. J. Biol. Chem 1991;266:4269–75. [PubMed: 1999419]
112. Nakayama TA, Khorana HG. Orientation of retinal in bovine rhodopsin determined by cross-linking using a photoactivatable analog of 11-*cis*-retinal. J. Biol. Chem 1990;265:15762–69. [PubMed: 2144289]
113. Lou J, Tan Q, Karnaukhova E, Berova N, Nakanishi K, Crouch RK. Synthetic retinals: convenient probes of rhodopsin and visual transduction process. Methods Enzymol 2000;315:219–37. [PubMed: 10736705]
114. Okada T, Kandori H, Shichida Y, Yoshizawa T, Denny M, et al. Spectroscopic study of the batho-to-lumi transition during the photobleaching of rhodopsin using ring-modified retinal analogues. Biochemistry 1991;30:4796–802. [PubMed: 2029520]
115. DeGrip WJ, Liu RS, Ramamurthy V, Asato A. Rhodopsin analogues from highly hindered 7-*cis* isomers of retinal. Nature 1976;262:416–18. [PubMed: 958397]
116. Kawamura S, Miyatani S, Matsumoto H, Yoshizawa T, Liu RS. Photochemical studies of 7-*cis*-rhodopsin at low temperatures. Nature and properties of the bathointermediate. Biochemistry 1980;19:1549–53. [PubMed: 7378362]
117. Shichida Y, Kandori H, Okada T, Yoshizawa T, Nakashima N, Yoshihara K. Differences in the photobleaching process between 7-*cis*- and 11-*cis*-rhodopsins: a unique interaction change between the chromophore and the protein during the lumi-meta I transition. Biochemistry 1991;30:5918–26. [PubMed: 1828372]
118. Buczylko J, Saari JC, Crouch RK, Palczewski K. Mechanisms of opsin activation. J. Biol. Chem 1996;271:20621–30. [PubMed: 8702809]
119. Jang GF, Kuksa V, Filipek S, Bartl F, Ritter E, et al. Mechanism of rhodopsin activation as examined with ring-constrained retinal analogs and the crystal structure of the ground state protein. J. Biol. Chem 2001;276:26148–53. [PubMed: 11316815]
120. Bhattacharya S, Ridge KD, Knox BE, Khorana HG. Light-stable rhodopsin. I. A rhodopsin analog reconstituted with a nonisomerizable 11-*cis* retinal derivative. J. Biol. Chem 1992;267:6763–69. [PubMed: 1551885]
121. Jang GF, McBee JK, Alekseev AM, Haeseleer F, Palczewski K. Stereoisomeric specificity of the retinoid cycle in the vertebrate retina. J. Biol. Chem 2000;275:28128–38. [PubMed: 10871622]
122. Ridge KD, Bhattacharya S, Nakayama TA, Khorana HG. Light-stable rhodopsin. II. An opsin mutant (TRP-265-Phe) and a retinal analog with a nonisomerizable 11-*cis* configuration form a photostable chromophore. J. Biol. Chem 1992;267:6770–75. [PubMed: 1532391]
123. Zhukovsky EA, Robinson PR, Oprian DD. Transducin activation by rhodopsin without a covalent bond to the 11-*cis*-retinal chromophore. Science 1991;251:558–60. [PubMed: 1990431]
124. McDowell JH, Williams TP. Oxidation states of four sulfurs of rhodopsin before and after bleaching. Vis. Res 1976;16:643–46. [PubMed: 960587]

125. Karnik SS, Khorana HG. Assembly of functional rhodopsin requires a disulfide bond between cysteine residues 110 and 187. J. Biol. Chem 1990;265:17520–24. [PubMed: 2145276]

126. Ernst OP, Hofmann KP, Sakmar TP. Characterization of rhodopsin mutants that bind transducin but fail to induce GTP nucleotide uptake. Classification of mutant pigments by fluorescence, nucleotide release, and flash-induced light-scattering assays. J. Biol. Chem 1995;270:10580–86. [PubMed: 7737995]

127. Franke RR, Konig B, Sakmar TP, Khorana HG, Hofmann KP. Rhodopsin mutants that bind but fail to activate transducin. Science 1990;250:123–25. [PubMed: 2218504]

128. Imamoto Y, Kataoka M, Tokunaga F, Palczewski K. Light-induced conformational changes of rhodopsin probed by fluorescent Alexa594 immobilized on the cytoplasmic surface. Biochemistry 2000;39:15225–33. [PubMed: 11106502]

129. Abdulaev NG, Ridge KD. Light-induced exposure of the cytoplasmic end of transmembrane helix seven. Proc. Natl. Acad. Sci. USA 1998;95:12854–59. [PubMed: 9789004]

130. Schertler GF, Hargrave PA. Projection structure of frog rhodopsin in two crystal forms. Proc. Natl. Acad. Sci. USA 1995;92:11578–82. [PubMed: 8524807]

131. Schertler GF, Hargrave PA. Preparation and analysis of two-dimensional crystals of rhodopsin. Methods Enzymol 2000;315:91–107. [PubMed: 10736696]

132. Schertler GF, Villa C, Henderson R. Projection structure of rhodopsin. Nature 1993;362:770–72. [PubMed: 8469290]

133. Davies A, Gowen BE, Krebs AM, Schertler GF, Saibil HR. Three-dimensional structure of an invertebrate rhodopsin and basis for ordered alignment in the photoreceptor membrane. J. Mol. Biol 2001;314:455–63. [PubMed: 11846559]

134. Pogozheva ID, Lomize AL, Mosberg HI. The transmembrane 7-alpha-bundle of rhodopsin: distance geometry calculations with hydrogen bonding constraints. Biophys. J 1997;72:1963–85. [PubMed: 9129801]

135. Baldwin JM, Schertler GF, Unger VM. An alpha-carbon template for the transmembrane helices in the rhodopsin family of G-protein-coupled receptors. J. Mol. Biol 1997;272:144–64. [PubMed: 9299344]

136. Altenbach C, Klein-Seetharaman J, Cai K, Khorana HG, Hubbell WL. Structure and function in rhodopsin: mapping light-dependent changes in distance between residue 316 in helix 8 and residues in the sequence 60–75, covering the cytoplasmic end of helices TM1 and TM2 and their connection loop CL1. Biochemistry 2001;40:15493–500. [PubMed: 11747424]

137. Meng EC, Bourne HR. Receptor activation: What does the rhodopsin structure tell us? Trends Pharmacol. Sci 2001;22:587–93. [PubMed: 11698103]

138. Dartnall HJA. The photosensitivities of visual pigments in the presence of hydroxylamine. Vis. Res 1968;8:339–58. [PubMed: 5315589]

139. Honig B, Ebrey T, Callender RH, Dinur U, Ottolenghi M. Photoisomerization, energy storage, and charge separation: a model for light energy transduction in visual pigments and bacteriorhodopsin. Proc. Natl. Acad. Sci. USA 1979;76:2503–7. [PubMed: 288039]

140. Cooper A. Energy uptake in the first step of visual excitation. Nature 1979;282:531–33. [PubMed: 503236]

141. Borhan B, Souto ML, Imai H, Shichida Y, Nakanishi K. Movement of retinal along the visual transduction path. Science 2000;288:2209–12. [PubMed: 10864869]

142. Jager F, Fahmy K, Sakmar TP, Siebert F. Identification of glutamic acid 113 as the Schiff base proton acceptor in the metarhodopsin II photointermediate of rhodopsin. Biochemistry 1994;33:10878–82. [PubMed: 7916209]

143. Farrens DL, Altenbach C, Yang K, Hubbell WL, Khorana HG. Requirement of rigid-body motion of transmembrane helices for light activation of rhodopsin. Science 1996;274:768–70. [PubMed: 8864113]

144. Kim JM, Altenbach C, Thurmond RL, Khorana HG, Hubbell WL. Structure and function in rhodopsin: rhodopsin mutants with a neutral amino acid at E134 have a partially activated conformation in the dark state. Proc. Natl. Acad. Sci. USA 1997;94:14273–78. [PubMed: 9405602]

145. Chen S, Lin F, Xu M, Hwa J, Graham RM. Dominant-negative activity of an alpha(1B)-adrenergic receptor signal-inactivating point mutation. EMBO J 2000;19:4265–71. [PubMed: 10944109]

146. Altenbach C, Cai K, Klein-Seetharaman J, Khorana HG, Hubbell WL. Structure and function in rhodopsin: mapping light-dependent changes in distance between residue 65 in helix TM1 and residues in the sequence 306–319 at the cytoplasmic end of helix TM7 and in helix H8. Biochemistry 2001;40:15483–92. [PubMed: 11747423]

147. Ernst OP, Meyer CK, Marin EP, Henklein P, Fu WY, et al. Mutation of the fourth cytoplasmic loop of rhodopsin affects binding of transducin and peptides derived from the carboxyl-terminal sequences of transducin alpha and gamma subunits. J. Biol. Chem 2000;275:1937–43. [PubMed: 10636895]

148. Marin EP, Krishna AG, Zvyaga TA, Isele J, Siebert F, Sakmar TP. The amino terminus of the fourth cytoplasmic loop of rhodopsin modulates rhodopsin-transducin interaction. J. Biol. Chem 2000;275:1930–36. [PubMed: 10636894]

149. Hamm HE. How activated receptors couple to G proteins. Proc. Natl. Acad. Sci. USA 2001;98:4819–21. [PubMed: 11320227]

150. Weitz CJ, Nathans J. Histidine residues regulate the transition of photoexcited rhodopsin to its active conformation, metarhodopsin II. Neuron 1992;8:465–72. [PubMed: 1532320]

151. Abdulaev NG, Ngo T, Chen R, Lu Z, Ridge KD. Functionally discrete mimics of light-activated rhodopsin identified through expression of soluble cytoplasmic domains. J. Biol. Chem 2000;275:39354–63. [PubMed: 10988291]

152. Baldwin PA, Hubbell WL. Effects of lipid environment on the light-induced conformational changes of rhodopsin. 2. Roles of lipid chain length, unsaturation, and phase state. Biochemistry 1985;24:2633–39. [PubMed: 4027218]

153. Rath P, DeGrip WJ, Rothschild KJ. Photoactivation of rhodopsin causes an increased hydrogen-deuterium exchange of buried peptide groups. Biophys. J 1998;74:192–98. [PubMed: 9449322]

154. Stenkamp RE, Filipek S, Driessen CAGG, Teller DC, Palczewski K. Crystal structure of rhodopsin: a template for cone visual pigments and other G protein-coupled receptors. Biochim. Biophys. Acta 2002;1565:168–82. [PubMed: 12409193]

155. Neitz M, Neitz J, Jacobs GH. Spectral tuning of pigments underlying red-green color vision. Science 1991;252:971–74. [PubMed: 1903559]

156. Stockman A, Sharpe LT, Merbs S, Nathans J. Spectral sensitivities of human cone visual pigments determined in vivo and in vitro. Methods Enzymol 2000;316:626–50. [PubMed: 10800706]

157. Merbs SL, Nathans J. Absorption spectra of human cone pigments. Nature 1992;356:433–35. [PubMed: 1557124]

158. Merbs SL, Nathans J. Absorption spectra of the hybrid pigments responsible for anomalous color vision. Science 1992;258:464–66. [PubMed: 1411542]

159. Nathans J. In the eye of the beholder: visual pigments and inherited variation in human vision. Cell 1994;78:357–60. [PubMed: 8062382]

160. Sharpe LT, Stockman A, Jagle H, Knau H, Klausen G, et al. Red, green, and red-green hybrid pigments in the human retina: correlations between deduced protein sequences and psychophysically measured spectral sensitivities. J. Neurosci 1998;18:10053–69. [PubMed: 9822760]

161. Merbs SL, Nathans J. Role of hydroxyl-bearing amino acids in differentially tuning the absorption spectra of the human red and green cone pigments. Photochem. Photobiol 1993;58:706–10. [PubMed: 8284327]

162. Asenjo AB, Rim J, Oprian DD. Molecular determinants of human red/green color discrimination. Neuron 1994;12:1131–38. [PubMed: 8185948]

163. Kochendoerfer GG, Kaminaka S, Mathies RA. Ultraviolet resonance Raman examination of the light-induced protein. Biochemistry 1997;36:13153–59. [PubMed: 9376376]

164. Marinissen MJ, Gutkind JS. G–protein-coupled receptors and signaling networks: emerging paradigms. Trends Pharmacol. Sci 2001;22:368–76. [PubMed: 11431032]

165. Gether U. Uncovering molecular mechanisms involved in activation of G protein-coupled receptors. Endocr. Rev 2000;21:90–113. [PubMed: 10696571]

166. Angers S, Salahpour A, Bouvier M. Dimerization: an emerging concept for G protein-coupled receptor ontogeny and function. Annu. Rev. Pharmacol. Toxicol 2002;42:409–35. [PubMed: 11807178]

167. Ballesteros JA, Shi L, Javitch JA. Structural mimicry in G protein-coupled receptors: implications of the high-resolution structure of rhodopsin for structure-function analysis of rhodopsin-like receptors. Mol. Pharmacol 2001;60:1–19. [PubMed: 11408595]

168. Brady JGP, Stouten PFW. Fast prediction and visualization of protein binding pockets with PASS. J. Comp.-Aided Mol. Des 2000;14:383–401.

169. Ballesteros J, Palczewski K. G protein-coupled receptor drug discovery: implication from the crystal structure of rhodopsin. Curr. Opin. Drug Disc. Dev 2001;4:561–74.

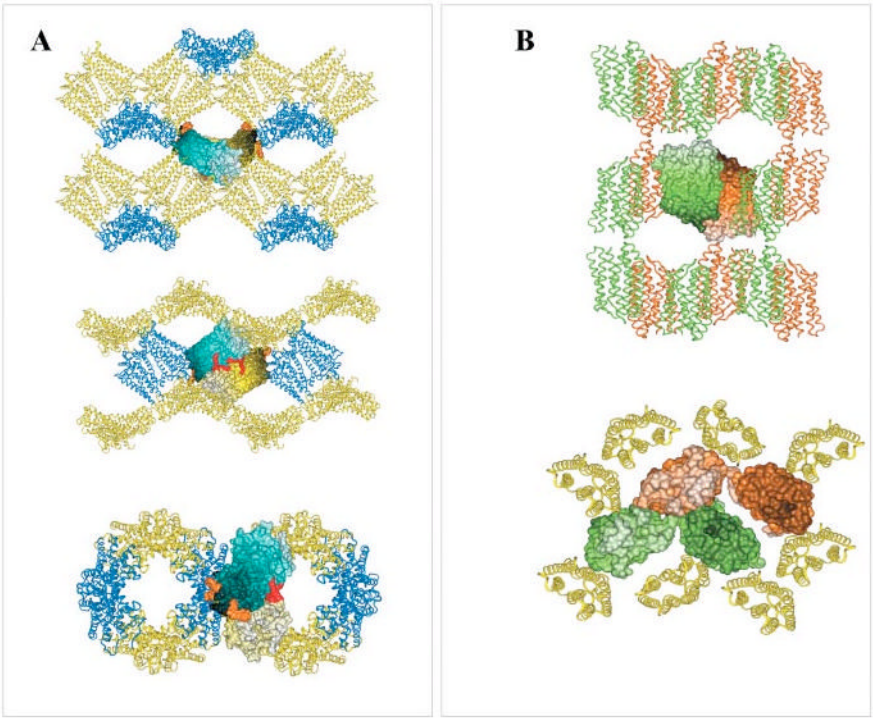

Figure 1.
Molecular packing of rhodopsin (*A*) and sensory rhodopsin (*B*) in their crystals. One asymmetric unit contains two rhodopsin molecules. The central dimer is shown as a continuous surface, whereas the rest are shown as ribbons. Views are from different crystallographic X-, Y-, Z-axes for rhodopsin (27), and X-, and Z- for sensory rhodopsin. The data for sensory rhodopsin were taken from Protein Data Base (1H68). Coordinates: Models of rhodopsin and the homology models of cone pigments have been deposited in the Protein Data Bank (PDB) (identifiers 1F88, 1HZX, 1KPN, 1KPW, 1KPX).

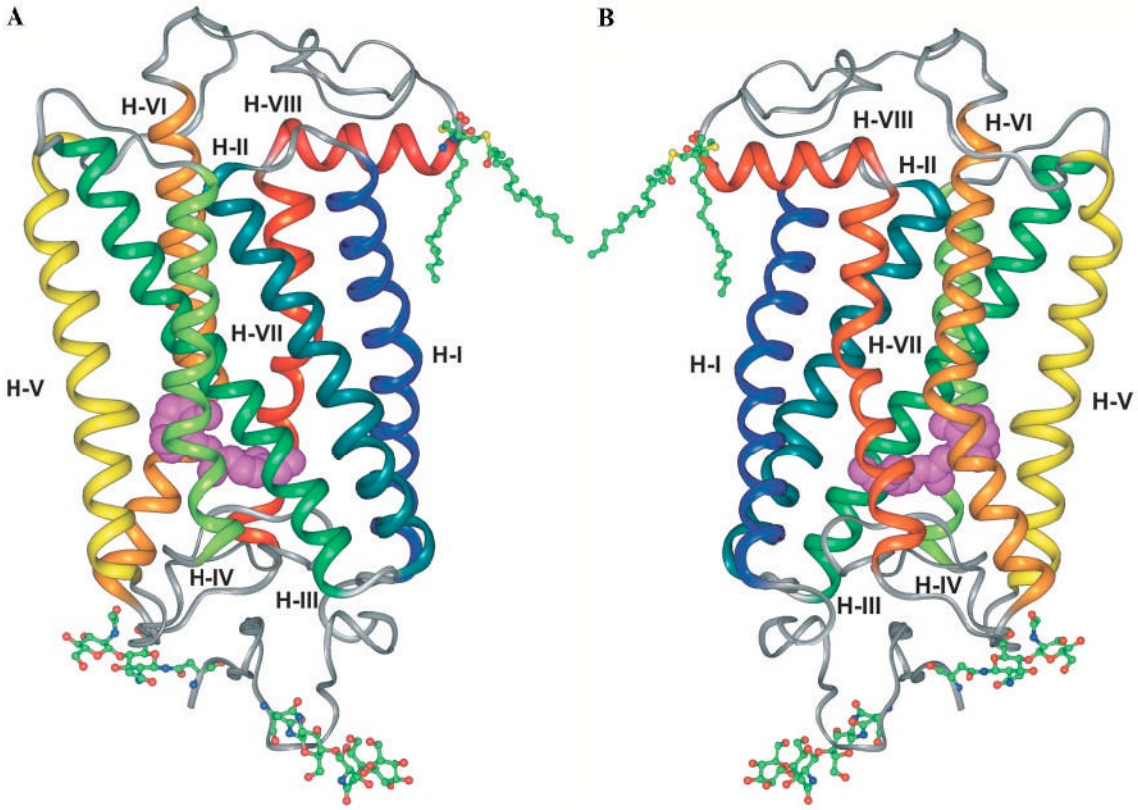

Figure 2.
Ribbon drawings of rhodopsin. Helices I–VIII are colored as a spectrum of visible light from blue (helix I) to red (helix VIII), and two orientations are shown. Palmitoyl chains and oligosaccharide groups shown using ball-and-stick models.

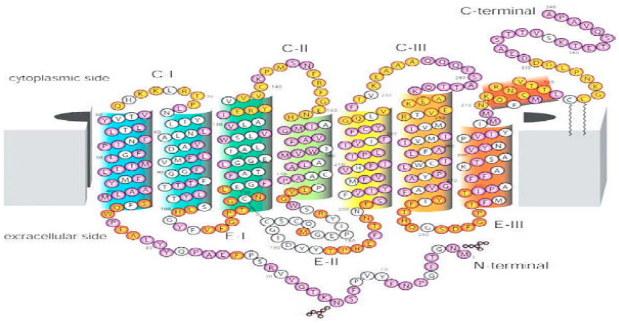

Figure 3.

Two-dimensional model of bovine rhodopsin. Buried residues are shown in gray. Orange, red, and violet denote surface residues. Residues in contact with polar headgroups of the membrane on the cytoplasmic side are orange. Similar residues on the extracellular side are red. All other surface residues are violet.

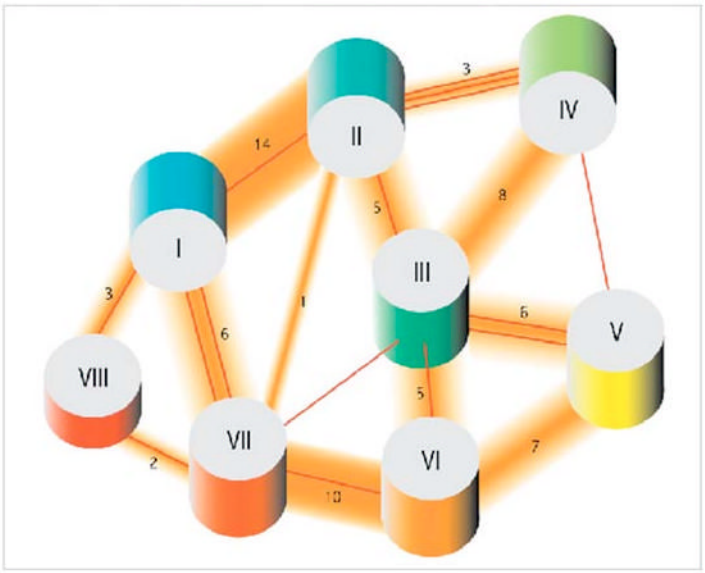

Figure 4.

Hydrophobic and hydrophilic interactions between rhodopsin helices (loops not included) viewed from the intracellular side. Hydrophobic interactions are shown as orange fuzzy bars together with numbers denoting their strength. Hydrophilic interactions are shown as red lines. List of hydrophilic interactions between helices include helices I–II, Asn^{55}-Asp^{83}; helices I–VII, Tyr^{43}-Phe^{293}, Asn^{55}-Ala^{299}; helices I–VIII, Gln^{64}-Thr^{320}; helices II–III, Asn^{78}-Ser^{127}; helices II–IV: Tyr^{74}-Glu^{150}, Asn^{78}-Thr^{160}, Asn^{78}-Trp^{161}; helices III–V, Cys^{140}-Thr^{229}, Glu^{122}-Trp^{126}-His^{211}-Tyr^{206} network; helices III–VI, Arg^{135}-Glu^{247}; helices III–VII, Glu113-Lys^{296} (retinal); helices IV–V, Ala^{166}-Tyr^{206}; helices VI–VII, Cys^{264}-Thr^{297}; and helices VII–VIII, Ile^{307}-Arg^{314}.

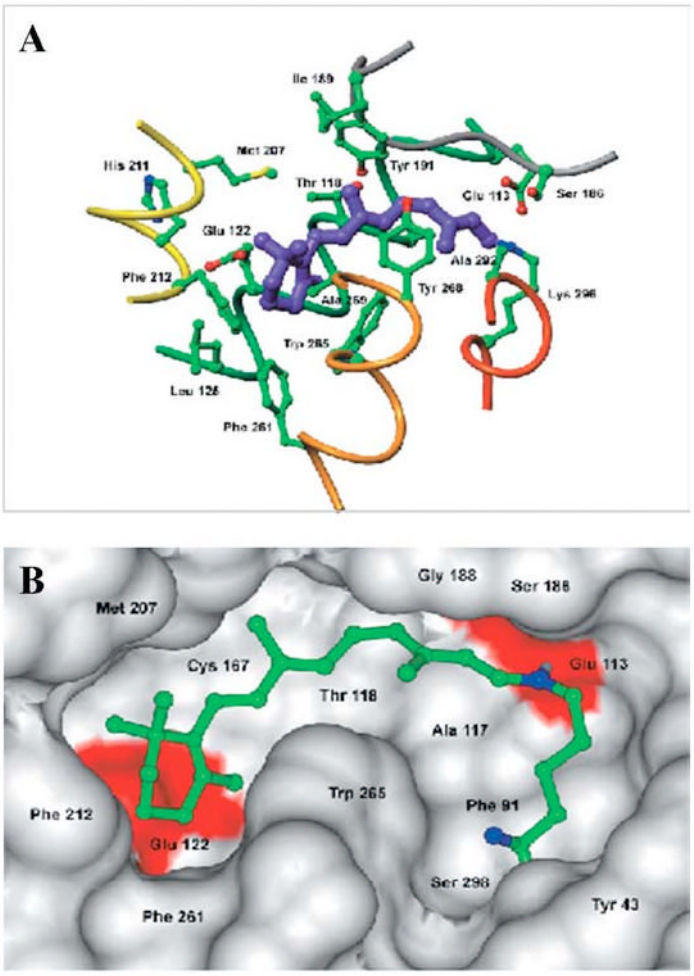

Figure 5.

Vicinity of retinal in the binding site of rhodopsin. (*A*) Chromophore-binding site of bovine rhodopsin. The chromophore is in purple, and colors of helices are as in Figure 2. (*B*) The structure of 11-*cis*-retinal bovine opsin (27) using space-filling model. In blue are nitrogen atoms of the peptide bond and the Schiff base, with the hydrogen between Lys^{296} and the retinal in green. In red, two acidic residues in the binding site, Glu^{113} and Glu^{122}, which is close to the β-ionone ring.

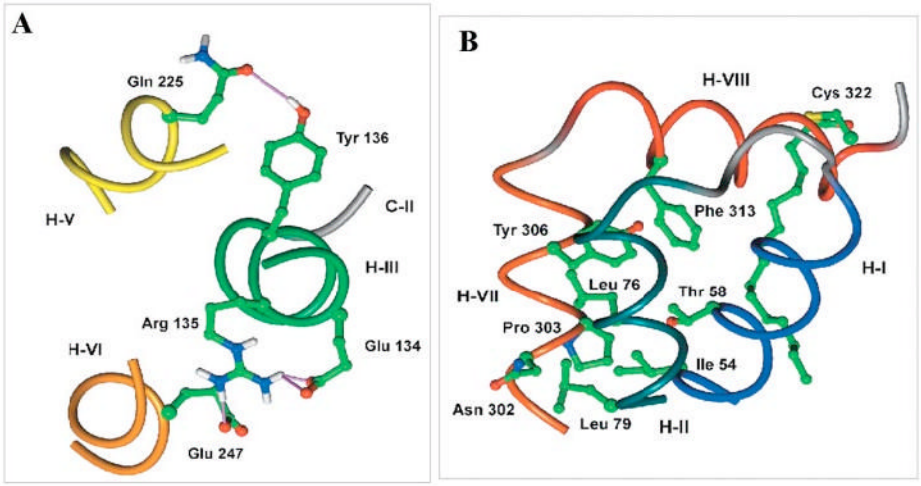

Figure 6.
The DRY region (*A*) and NPXXY region (*B*) are believed to be involved in the activation and transformation of photoactivated rhodopsin. Note that in rhodopsin, the sequence of the DRY region is ERY.

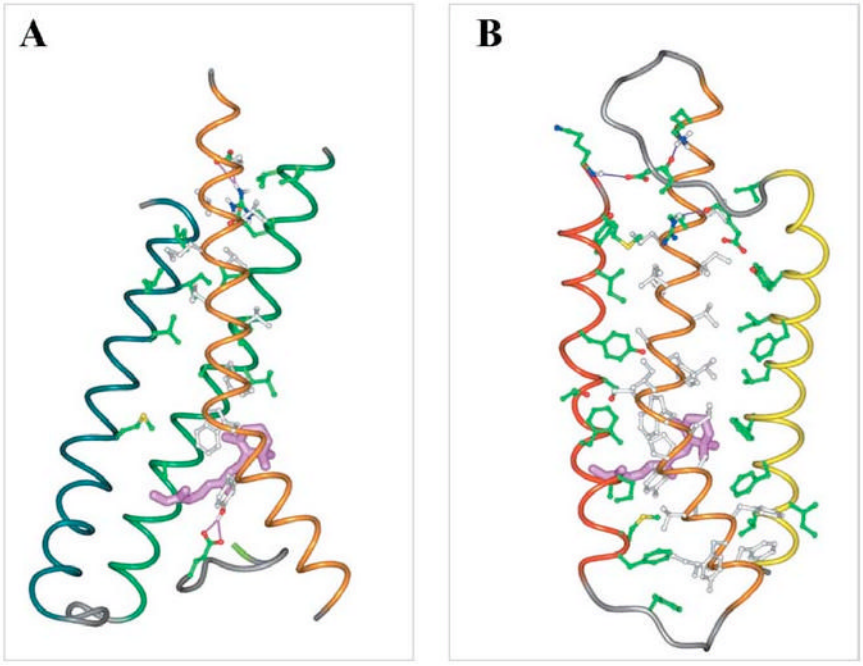

Figure 7.
Interactions of helix VI. Hydrophobic contacts of helix VI shown as white residues and hydrophilic interactions represented by lines. (*A*) Interaction of helix VI with helices II and III. (*B*) Interaction of helix VI with helices V and VII.

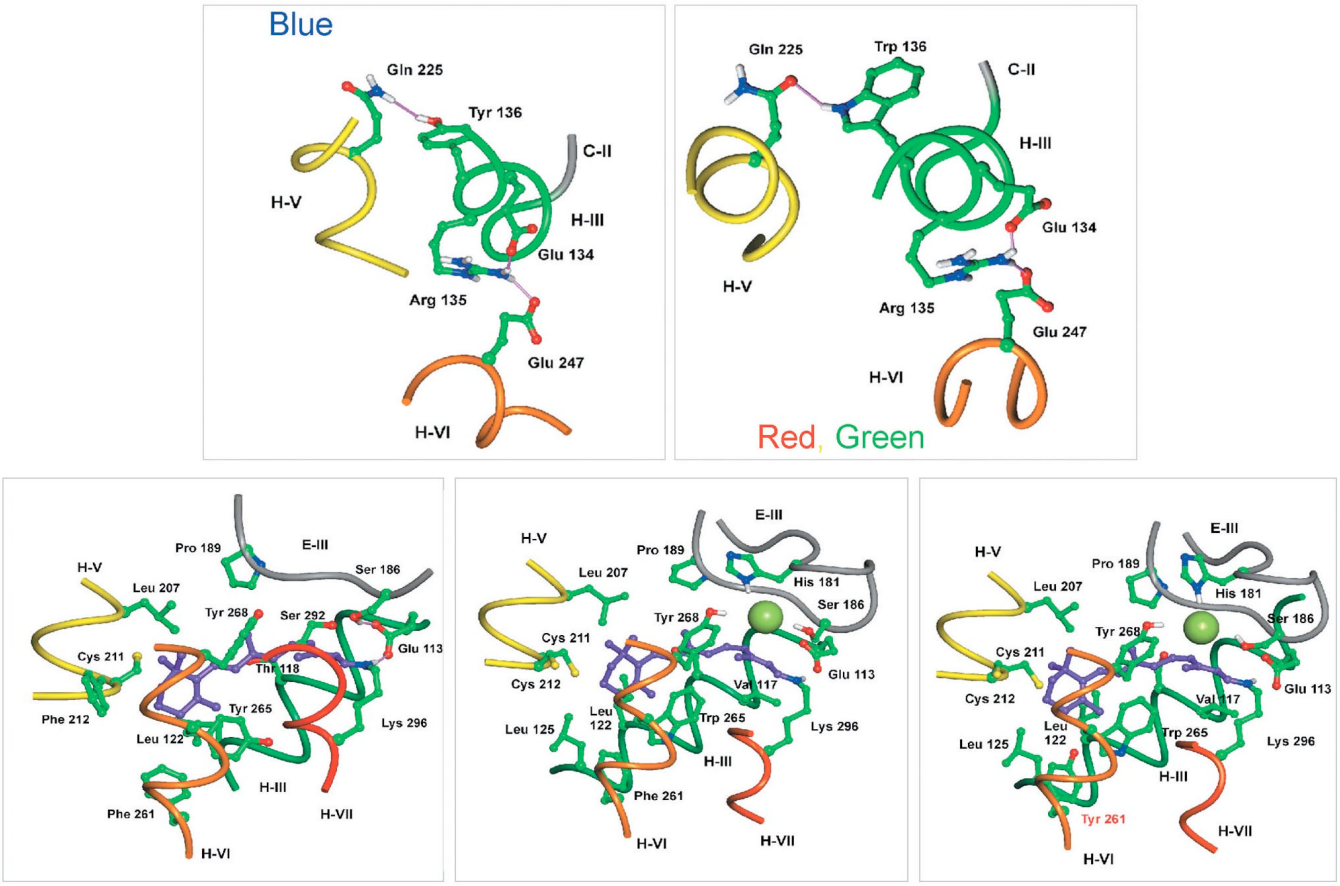

Figure 8.

Different regions of cone pigments. (*A*) DRY region and the chromophore-binding sites of blue and red/green cone opsins. (*B*) The vicinity of the chromophore from left to right: blue, green, and red pigments. The numbering of corresponding regions is based on the bovine rhodopsin primary sequence.

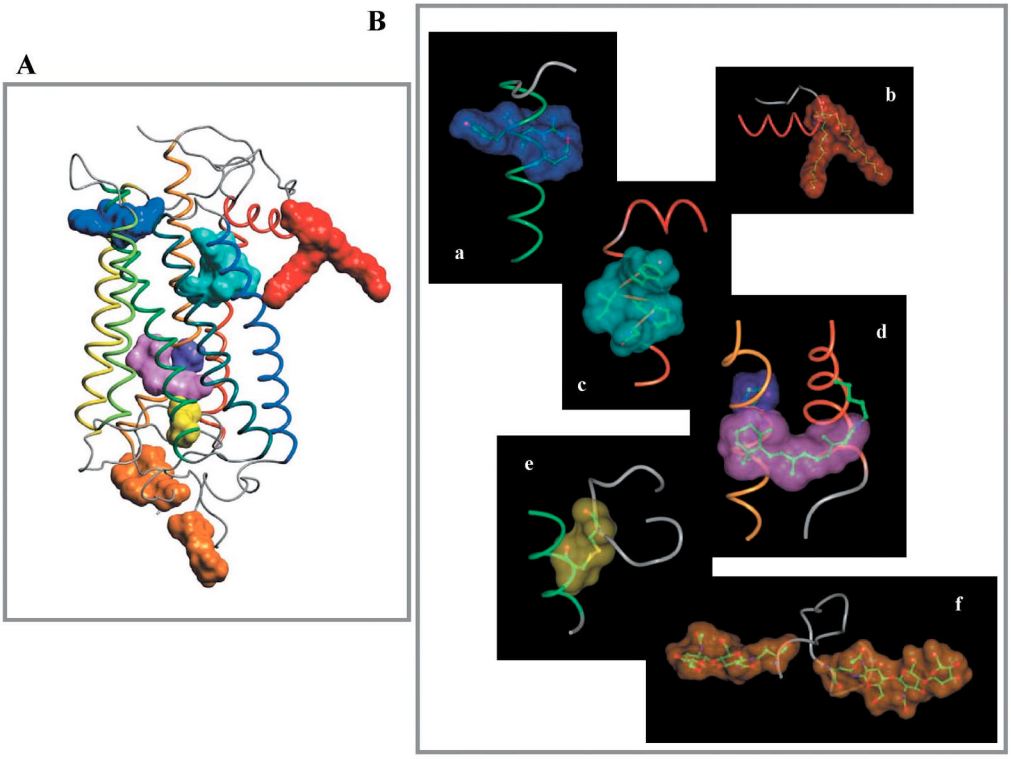

Figure 9.
Functional domains of rhodopsin that are highly conserved among members of the GPCR superfamily. (*A*) Location of these domains in the three-dimensional structure of rhodopsin. (*B*) Close-up of the critical regions: DRY region (*a*, *panel A*, in rhodopsin ERY, blue); palmitoyl groups (*b*, *panel A*, red); NPXXY region (*c*, *panel A*, light blue); chromophore; Pro kink in helix VI, Lys^{296} (*d*, *panel A*, violet); disulfide bridge (*e*, *panel A*, yellow); and oligosaccharide moieties (*f*, *panel A*, brown).